The design and analysis of a prototype concentrated solar power installation with PV cells

Maciej Jakub Szram

Thesis to obtain the Master of Science Degree in

Energy Engineering and Management

Supervisors: Prof. Pedro Jorge Martins Coelho

Dr Krzysztof Sornek

Examination Committee

Chairperson: Prof. Edgar Caetano Fernandes

Supervisor: Prof. Pedro Jorge Martins Coelho

Member of the Committee: Prof. Luís Filipe Moreira Mendes

July 2022

I declare that this document is an original work of my own authorship and that it fulfills all the requirements of the Code of Conduct and Good Practices of the Universidade de Lisboa.

Acknowledgements

I would first like to thank my thesis supervisor Professor Pedro Jorge Martins Coelho of the University of Lisbon, Instituto Superior Tecnico for continuous support and guidance on concentrated solar power. I would also like to thank Doctor Krzysztof Sornek for his invaluable help in the construction of the concentrated photovoltaic thermal collector and his guidance in the field of photovoltaics.

I am sincerely grateful to Doctor Karol Sztekler for encouraging me to join the InnoEnergy Masters Degree Program and providing help during my master studies.

Abstract

The rise of energy demand and the need to decrease carbon dioxide emissions worldwide led to a rapid development of renewable energy technologies, including solar energy systems. Concentration solar technologies, such as Concentrated Solar Power (CSP) and Concentrated Photovoltaics (CPV) have also gained scientific interest. A concentrating photovoltaic thermal (CPVT) collector uses a concentrated beam of light to generate useful heat and electricity simultaneously. In frames of the thesis, a prototype parabolic trough type CSP installation with PV cells attached to the receiver (CPVT collector) has been built and its performance has been analyzed. The influence of different types of PV cells on the energy output has been investigated. Data was collected using multimeters, pyranometers, thermocouples and an infra-red camera. The results obtained in this study have been compared with literature and potential improvements of the system have been proposed. Under concentrated irradiance monocrytalline silicon and amorphous silicon cells achieved 13,54±0,24% and 7,69±0,14% electrical efficiency respectively. The thermal efficiency of the system was equal to 77,20±6,09%.

Keywords: renewable energy, solar energy, concentrating solar power, concentrating photovoltaics,

Resumo

O aumento da procura de energia e a necessidade de diminuir as emissões de dióxido de carbono em todo o mundo levaram a um rápido desenvolvimento de tecnologias de energia renovável, incluindo sistemas de energia solar. As tecnologias solares de concentração, como a Energia Solar Concentrada (CSP) e a Fotovoltaica Concentrada (CPV), também ganharam interesse científico. Um coletor térmico fotovoltaico concentrado (CPVT) usa um feixe de luz concentrado para gerar calor útil e eletricidade simultaneamente. No âmbito desta, foi construído um protótipo de instalação de calha parabólica tipo CSP com células fotovoltaicas acopladas ao receptor (coletor de CPVT) e o seu desempenho foi analisado. A influência de diferentes tipos de células fotovoltaicas na produção de energia foi investigada. Os dados foram coletados usando multímetros, piranometros, termopares e uma camara infravermelha. Os resultados obtidos neste estudo foram comparados com outros disponí veis na literatura e foram propostas melhorias potenciais do sistema. Sob irradiância concentrada, as células de silício monocristalino e de silício amorfo alcançaram 13,54±0,24% e 7,69±0,14% de eficiência elétrica, respectivamente. A eficiência térmica do sistema foi igual a 77,20±6,09%.

Palavras-chave: energia renovável, energia solar, energia solar concentrada, energia fotovoltaica concentrada

Table of Contents

List of Figures

List of Tables

1. Introduction

1.1 Problem statement

Since the energy sector is responsible for a significant portion of greenhouse gases emitted to the atmosphere, clean ways of energy harvesting need to be developed and improved. Solar energy systems are on the rise and concentrating solar systems offer valuable advantages. The problem addressed in this thesis is the design and construction of a relatively simple Concentrated Photovoltaic Thermal (CPVT) installation with satisfactory efficiency and energy output.

1.2 Motivation

Climate change leads to a significant number of negative results, including water and food scarcity and irreversibly changing natural habitats all over the world, among many others. Since the effects of climate changes are becoming more visible each year, numerous countries and associations try to implement solutions to the problem. According to the Paris Agreement – an international treaty on climate change, energy transition is necessary to mitigate these harmful effects. The main goal of the agreement is to prevent the average ambient temperature from increasing by more than 1,5°C – when compared to the pre-industrial era [1].

Various industries affect the environment, however, one of the main sectors contributing to climate change is heat and electricity generation. The impact each sector has on the environment is often measured by the amount of greenhouse gases (GHG) emitted [2]. The chart displayed in Figure 1 was created based on the data shared by Environmental Protection Agency and shows how each sector contributes to GHG emissions [3].

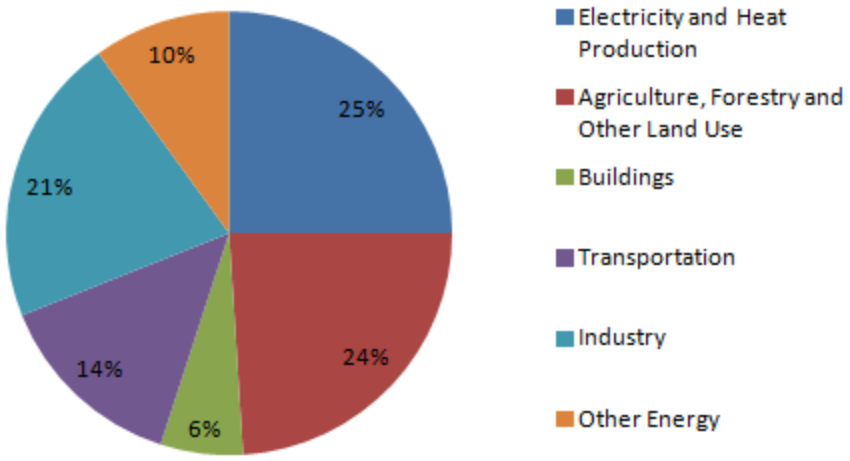

Figure 1. Worldwide GHG emissions by sector [3]

Even though one often refers to carbon dioxide as the main GHG, it is not the only one emitted in large quantities. Another gas contributing to global warming is methane, whose warming potential is twenty one times greater than CO_2 and there are many other gases with even greater warming potentials [2]. The data for Figure 1 took into account all GHG and their warming potentials and the results show that electricity and heat production has the greatest contribution to climate change. Yet, the influence of other sectors, such as Agriculture, Industry and Transportation is not negligible.

International Renewable Energy Agency (IRENA) estimates that 33 billion dollars will need to be invested in photovoltaic and hydrogen technologies, as well as electromobillity until 2050 [4]. As much as 14 TW of solar power needs to be installed by the end of 2050 [4]. GHG emissions from the energy sector need to be reduced significantly – since effects of global warming are alarming, such as abnormally high ground temperatures [5].

Among other renewable energy sources, it is the solar energy that will most likely experience the greatest rise in the years to come. As of today, the utility scale photovoltaic electricity generation is the cheapest way to produce electricity [6]. In order to investigate the economic aspects of energy technologies, usually Levelized Cost of Energy (LCOE) for each technology is compared. LCOE is a measure of the average net present cost of energy production for a power plant over its lifetime [6]. Figure 2 compares LCOE for each technology in 2021:

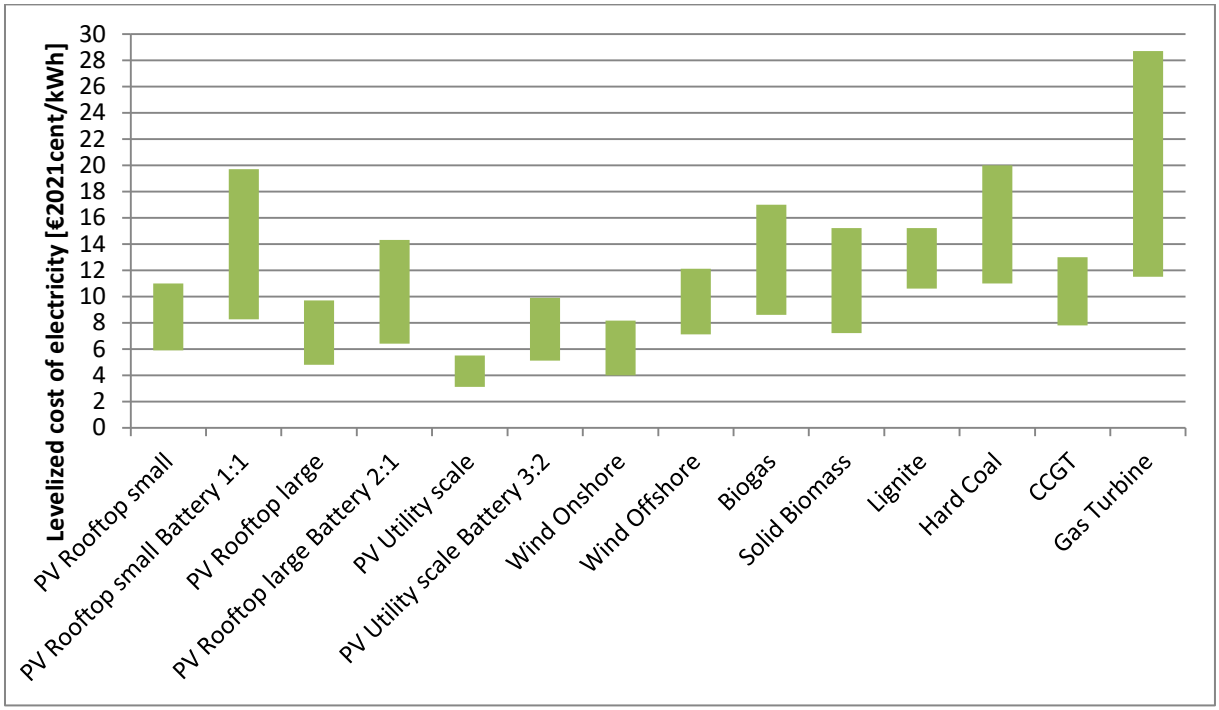

Figure 2. LCOE for energy technologies in 2021 [6]

As shown in Figure 2, currently utility scale PV has the lowest LCOE of all energy technologies. This is a reason, why large scale solar parks become more and more popular in countries all over the world.

In many countries around the world, including Poland, photovoltaics has already taken a leading role in the Renewable Energy industry when it comes to the number of new projects being built each year. IRENA estimates that by the end of 2050, solar energy industry will have hired 42,5 million employees worldwide [4].

Thus, by the end of 2050 sun will most likely become the most important energy source, leaving fossil fuels, nuclear energy and even other renewable energy sources behind. And even though traditional photovoltaic technologies seem the most prosperous, there is a great interest in concentration technologies too. Some studies show, that Concentrated Solar Power (CSP) can become more significant as the investment cost reduce [7].

In recent years, a number of projects focusing on Concentrating Solar Power were started. This includes the CAPTure project – dedicated to developing a highly efficient solar power station, or ORC-PLUS project, which developed an energy storage system for a medium size CSP installation among

many others [8]. These projects have received a great support from the European Union. The details of solar technologies will be discussed in the following chapters of the thesis.

Taking into account all the problems resulting from global warming, the prosperity of solar technologies and potential in concentrating solar technologies, concentrating solar energy systems were chosen as the topic of this thesis.

1.3 Objectives and methodology

The purpose of the thesis is to design, build and analyze the performance of a prototype CPVT collector. The goal is to have a complete data set of efficiency and electrical energy and useful heat generated by the installation. The aim is to understand how the implemented solutions affect the performance of the system and what potential improvements can be applied to enhance the energy output of the CPVT collector. Furthermore, the installation constructed for the purpose of the thesis can potentially become valuable for further research.

The process of conducting research was done as follows: First the key elements of the CPVT installation were designed and assembled. A concentrator was profiled using a TracePRO software. The concentrator was then assembled and mounted onto a structure. Later, the receiver which consisted of an aluminium duct with attached solar cells was prepared. Solar cells were first tested individually, then in proper connections and attached to the duct using thermally conductive adhesive. Then the receiver was installed in the focus of the concentrator and water hosepipes were attached. Data on electrical and thermal parameters of the installation under various conditions was collected using dedicated equipment. Finally, data was analyzed and the results were presented.

The work conducted in the thesis was done in line with the work of other researchers investigating low concentration CPVT systems. Most common types of solar cells were used similar way of constructing the installation was implemented.

1.4 Thesis outline

The thesis consists of four major chapters.

The first chapter describes state of the art and the theoretical background of the solar energy, with a strong emphasis put on concentration systems.

The second chapter focuses on the design of the CPVT installation. Elements and materials used, as well as their preparation are described in detail. Also, the instrumentation used in the measurements is described.

In the third chapter the experimental methodology applied in the process, as well as the experimental part are described. Detailed information regarding the measured parameters, methods used for their determination, as well as the results with comments can be found in this chapter.

In the final chapter, the main conclusions and final thoughts are presented.

2. Solar technologies and CPVT

2.1 Introduction to solar energy systems

Solar energy is a very universal form of energy, since solar irradiance can be relatively easily converted into heat or electricity, as well as used in chemical and biological processes. Solar energy devices are used in heating and cooling systems and technological processes. The examples of such processes are water desalination or biomass drying process, used to obtain hot water. Solar energy devices however vary significantly depending on their technological application [9].

2.1.1 Solar panels

The most commonly used solar energy devices are solar panels (assembled by connecting a number of solar cells) and solar thermal collectors. Whilst solar panels generate electricity, solar collectors generate heat (usually in a form of hot water) [10].

Solar cells convert solar energy into electricity using the photovoltaic effect. Photovoltaic effect can be described as a phenomenon where, due to solar irradiance, electric charges move and electromotive force is generated. Electromotive force, which is equal to the difference between the potentials of the electrodes, is created due to a stream of carriers flowing through the p-n junction [9]. Photovoltaic effect occurs in solids, liquids and gases but the highest rate of conversion is observed in semiconductors. Solar cells can be made of various semiconductors (such as amorphous silicon, CIGS, CdTe), however the most commonly used material is crystalline silicon – around 90% of all commercially used cells are made out of this material [11]. Figure 3 presents a schematic diagram of a silicon-based solar cell.

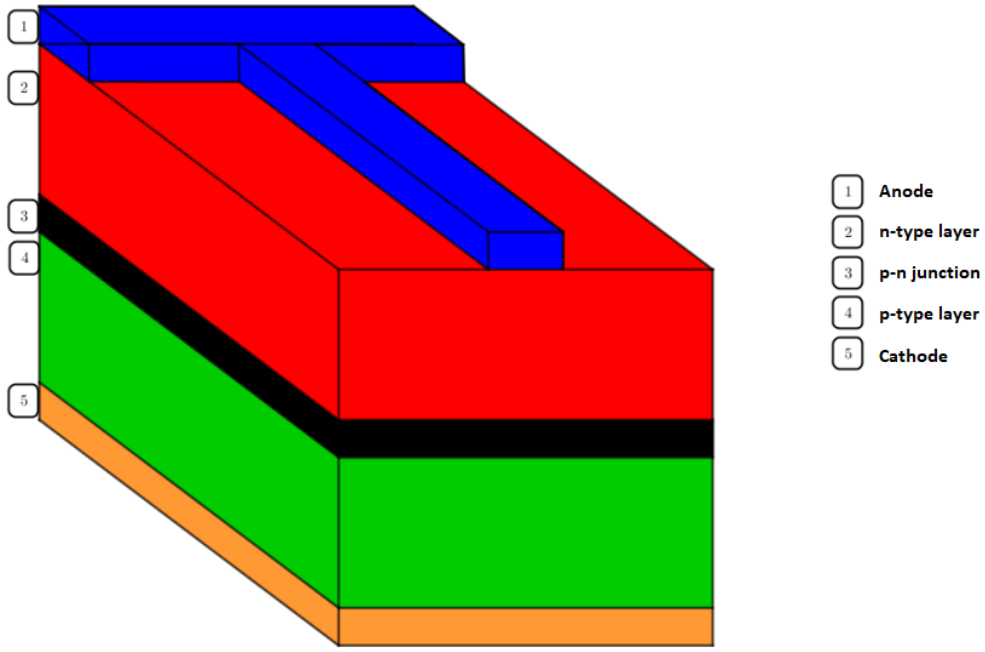

Figure 3. Solar cell schematic diagram [12]

Solar cell consists of two layers of crystalline silicon - a negative n-type layer and a positive p-type layer. In the n-type layer, which is usually doped with phosphorous atoms, electrons play a role of charge carriers. In the p-type layer (usually doped with boron atoms), holes are the charge carriers. A

positive electrode is attached to the p-type layer, and a negative electrode is attached to the n-type layer. Between these two layers, electrons can move freely through the p-n junction. In the case of direct band gap materials, such as amorphous silicon, when a photon, whose energy exceeds the band gap energy hits the cell, it can be absorbed and create a hole-electron pair. In the case of indirect band gap materials, like crystalline silicon, in order to create a hole-electro pair, the electron needs to receive enough energy from the photon, as well as enough momentum from the crystal. The electron is drawn to the negatively charged side, whilst the hole is drawn to the positively charged side. The electrons can flow through an electric circuit and do electrical work, such as lighting a bulb. Having done the electric work, the electrons return to the cell and recombine with previously created holes [13].

Even though various materials can be used to manufacture solar cells, silicon cells are the most popular and the silicon technologies will be of paramount importance for the thesis. One can distinguish polycrystalline silicon, monocrystalline silicon and amorphous silicon – and only the latter two will be analyzed in detail in the thesis.

The main difference between monocrystalline silicon and amorphous silicon is the structure of the silicon atoms. Amorphous silicon is a non-crystalline form of silicon, which means that atoms do not form any crystalline lattice. There is no symmetric pattern in their structure. Monocrystalline silicon atoms on the other hand form crystals with a regular pattern. The efficiency of amorphous silicon cells is much lower (around 6%) than monocrystalline silicon cells (15-20%). However, since only a thin layer of amorphous silicon is needed for power generation, the use of a-Si could potentially be economically justified in the future [11]. For these reasons, these two types of cells will be investigated in this thesis.

Structures of monocrystalline and amorphous silicon are shown in Figure 4.

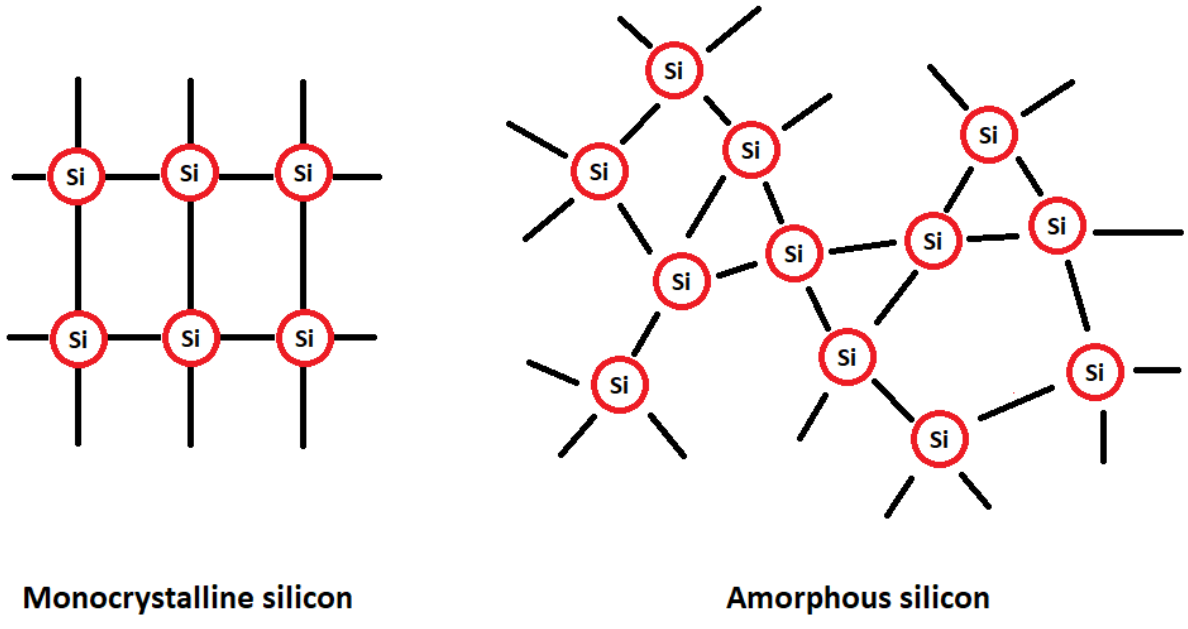

Figure 4 Monocrystalline and amorphous silicon structure [14]

Solar cells can be connected in series and in parallel in order to form a solar panel. Connecting the cells leads to the increase of generated current and/or voltage to a usable range. However solar cells form only one of the layers of solar panels. Apart from solar cells, solar panels usually contain two

layers of ethylene vinyl acetate (one on each side of the solar cells) – which protect the cells from humidity, dirt and mechanical damage, an electro-insulating foil sheet on the bottom, and a glass cover on the top. All of these sheets are then framed with an aluminum frame [15].

Solar panels can use various types of solar cells, however the majority of panels available commercially are based on crystalline silicon technology [11]. Figure 5 presents a view on solar panels with monocrystalline silicon cells.

Figure 5. Solar panels at AGH UST in Cracow, Poland

There is a number of important parameters which determine the operation of a solar cell or a solar panel. The most important parameters, relevant to the thesis are as follows: short circuit current, open circuit voltage, output power and efficiency. These parameters are briefly described below.

While analyzing electrical parameters of solar cells and solar panels, it is recommended to visualize the values using current-voltage and power curves. Current-voltage curves, also known as I-V curves are graphical representations of a relationship between the current and the voltage of a cell/panel. Power curves on the other hand show the relationship between the power and the voltage of a device [16].

Short circuit current is the current flowing through the solar cell when the cell is short circuited. In such a situation, the voltage across the solar cell is equal to zero. It is thus the maximum current that can flow through the cell at given conditions. Short circuit current is usually written as I_{sc} [16].

Open circuit voltage is the voltage from a cell occurring when there is no current flowing – the current is equal to zero. Therefore it is the maximum value of voltage that can be achieved under given conditions. Open circuit voltage is usually written as V_{oc} [16].

Output power is the amount of electrical power generated by a cell. The amount of power depends on both voltage and current. There is one particular point on the I-V curve, at which the power generated is the highest. This point is called the maximum power point. The power at maximum power point can be calculated using the Equation 1 [16]:

$$P_{MP} = U_{MP} \cdot I_{MP} \quad (1)$$

Where:

P_{MP} – Maximum electrical power output at maximum power point [W]

U_{MP} – Output voltage at maximum power point [V]

I_{MP} – Output current at maximum power point [A]

Electrical efficiency can be defined as the ratio of electrical power generated by the solar cell to the power delivered to the cell by the sun. Equation 2 can be used to calculate the efficiency of a solar cell or a solar panel [16]:

$$\eta_{el} = \frac{\mathrm{P_{MP}}}{\mathrm{G \cdot A}} \cdot 100\% \qquad (2)$$

Where:

η_{el} – Electrical efficiency [%]

P_{MP} – Maximum electrical power output at maximum power point [W]

G – Irradiance [W/m^2]

A – Cell area or Panel area [m^2]

It is also important to note, that the above-mentioned parameters depend on the conditions at which the cell operates. Since throughout the live cycle of a solar cell/panel it operates under a wide range of conditions, there needs to be a universal way to compare devices between one another. Thus, usually solar cells and panels manufacturers report the values of these parameters under Standard Test Conditions (STC) in the data sheets of their products [15].

Standard Test Conditions are defined by three main parameters. Solar irradiance for STC is equal to 1000 W/m^2. Furthermore, the temperature of the solar cell has to be equal to 25°C. The third and final determinant of STC is the Air Mass of 1.5. This parameter refers to the atmosphere thickness. Air Mass of 1.5 roughly corresponds to the atmosphere thickness the sunlight needs to pass through to reach a solar cell located in Europe [11].

In reality however, solar panels rarely operate under STC outside a lab. Thus sometimes, in order get information about the performance outside a lab, the following conditions are used as reference: Solar irradiance of 800 W/m^2, wind velocity of 1 m/s and the ambient temperature of 20°C [17]. The Nominal Operating Cell Temperature is the temperature of the solar panel under above-mentioned conditions. Some manufacturers include the information about I_{sc}, V_{oc}, P_{max} and η_{el} for NOCT alongside with values for STC.

Equation 3, which refers to NOCT can be used to calculate the temperature of the solar panel at different temperature and solar irradiance:

$$T_{cell} = T_{ambient} + \frac{G \cdot (NOCT - 20°\mathrm{C})}{800\,\frac{W}{m^2}} \qquad (3)$$

Where:

T_{cell} – Cell temperature [°C]

$T_{ambient}$ – Ambient temperature[°C]

G – Irradiance [W/m^2]

NOCT – Normal Operating Cell Temperature [°C]

However, under any other conditions, electrical parameters need to be measured individually. Alternatively, they can also be calculated using various mathematical models, which is however beyond the scope of the thesis.

2.1.2 Solar collectors

Another widely used device is a solar thermal collector. Solar collectors are used to convert solar energy into useful heat, often in a form of hot water. Figure 6 shows a schematic diagram of a flat solar collector [18].

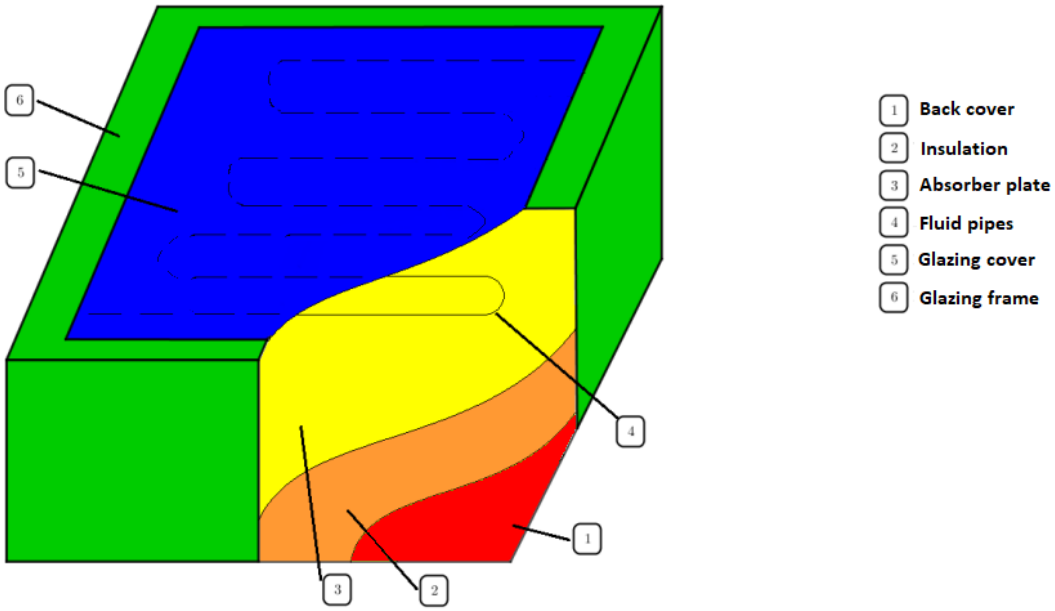

Figure 6. Flat solar collector schematic diagram

Absorber, glazing and insulation are key parts of a solar collector. Absorbers are usually made of aluminum or copper, and their purpose is to absorb as much irradiance as possible. Glazing covers the device and should be resistant to mechanical damage and sunlight. Furthermore, it should be made of a transparent material – thus often polytetrafluoroethylene (known as Teflon) is used. Insulation is used to reduce heat losses through convection, conduction and radiation. Commonly used materials for insulation are porous ebonite, porous polystyrene and cork [18].

Working fluid (usually water or glycol solution) flows through the fluid pipes and heats up by receiving heat from the absorber. The heat is then stored in a storage tank and can be used later in a variety of applications.

Figure 7 presents an operating flat solar collector installed on the rooftop of a household.

Figure 7. Solar collector in California, USA [19]

The amount of thermal power generated by the device is the power absorbed by the working fluid flowing through the system. It can be calculated using Equation 4:

$$\dot{Q} = c \cdot \dot{m} \cdot \Delta T \tag{4}$$

Where

$\dot{Q}$ – Thermal power [W]

c - Specific heat of the working fluid [J/(kg•°C)]

$\dot{m}$ – Mass flow rate [kg/s]

ΔT – Temperature difference [°C]

In order to determine thermal efficiency of the device, one has to compare the amount of thermal power to the amount of solar power delivered to the device by the sun. It can be with Equation 5:

$$\eta_{th} = \frac{\dot{\mathrm{Q}}}{\mathrm{G} \cdot \mathrm{A}} \cdot 100\% = \frac{\dot{\mathrm{Q}}}{\mathrm{P_{solar}}} \cdot 100\% \tag{5}$$

Where:

η_{th} – Thermal efficiency [%]

$\dot{\mathrm{Q}}$ – Thermal power [W]

G – Irradiance [W/m^2]

A – Collector area [m^2]

P_{solar} – Power delivered by the sun [W]

These are not the only technologies used – and different types can be distinguished within solar cells and solar collectors. Because of the fact that there is a plethora of devices available, some kind of classification is necessary. Devices can be grouped based on the type of energy generated: e.g. heat or electricity. Another classification can be named based on the location of the device – whether it is used on the Earth or in space. One can also distinguish different systems taking into account their orientation to the sun – whether the sun tracking system is used or not [9].

There is a number of other classifications, which are beyond the scope of this work. Nevertheless, the classification which is the most relevant to this thesis, is whether the device uses non-concentrated or concentrated solar irradiance.

Unlike regular solar devices operating under non-concentrated irradiance, concentrated solar systems use sets of mirrors or lenses to concentrate a beam of solar radiation into a given area so as to produce various forms of useful energy, such as electricity or heat [20]. This thesis' focus will be laid on technologies which use concentrated solar irradiance and they will be discussed in detail in succeeding chapters.

2.2 Concentrating Solar Technologies

Concentrating solar technologies use devices to focus sunlight at a specific area in order to generate energy. Amongst concentrated solar technologies there is a distinction between concentrated photovoltaics and concentrated solar power.

2.2.1 Concentrated photovoltaics

Concentrated photovoltaics, usually abbreviated as CPV, is a type of photovoltaic energy system, that uses lenses, curved mirrors and other types of optical instruments to concentrate a big amount of solar irradiance at a small area of a solar cell to generate electrical energy. In comparison to conventional photovoltaic technology, CPV systems allow to save money on solar cells, since a smaller area of the photovoltaic materials is required. Because of that, more expensive multi-junction solar cells can be used in CPV systems due to their high efficiency [21].

In order to concentrate light at a chosen area, concentration systems however require greater investments in solar trackers, cooling systems and concentrator optics. It is because of these additional costs that CPV systems are much less common than conventional photovoltaic technology. Currently, a lot of research is being done to decrease the overall costs of CPV systems [21].

Concentrated photovoltaic systems use either lenses or curved mirrors to concentrate light, however the former are more commonly used [22]. In order to focus light at a given area effectively, lenses used in CPV systems are spherical. For CPV applications normal lenses would have to be very thick. These lenses would be relatively expensive and have a relatively high optical absorption. Therefore, Fresnel lenses are generally used [22]. Fresnel lenses is a design that allows the construction of large aperture lenses and a short focal length without the weight and the bulk of material that is used in conventional lenses [22].

Alternatively to refractive lenses, curved mirrors can also be used. Any type of a reflective surface with a parabolic shape will focus parallel sun rays into a focus. CPV systems may use either parabolic dishes or parabolic troughs – however the latter are much more commonly used in CSP systems.

Optical collectors in CPV systems – lenses and mirrors – can only effectively concentrate direct light and most of the diffuse light is not used. Thus CPV systems require a tracking system to follow the sun's path through the sky. Two types of tracking systems can be distinguished: single axis and dual axis.

Systems which use parabolic troughs are usually equipped with single axis solar tracker, so a collector can only rotate along the focus line. However, when point-focus optics are used, a two-axis tracking

system is required. In such systems in order to follow the sun more accurately, both the azimuth and the tilt angle of the panel can be modified.

Figure 8 shows a concentrated photovoltaics dish system. In each unit light is concentrated at a cell located above the dish centre.

Figure 8. Concentrated photovoltaics dish system at Pitjantjatjara, Australia [20]

Another important aspect of a CPV system is the light concentration 'C'. This factor describes what the irradiance in the system is, compared to non concentrated 1 sun irradiance. Thus, when the light concentration is equal to 500, it means that in the system, the irradiance is 500 times higher than regular sun's 1000 W/m^2. When lenses are used, the light concentration 'C' is usually between 300 and 800 suns. For systems using mirrors to concentrate the light, the concentration can even go up to 1500 suns.

Optical concentration can be defined as the ratio of irradiance at the receiver surface to the incident solar irradiance. Furthermore, since one can assume that the short circuit current increases linearly with the increase of irradiance, the optical concentration C can also be calculated as a ratio of I_{sc} under concentrated irradiance to I_{sc} under 1-sun irradiance. Optical concentration can thus be expressed with Equation 6:

$$C = \frac{G_{concentrated}}{G_{1sun}} = \frac{I_{sc,\ concentrated}}{I_{sc,\ 1sun}} \quad (6)$$

Where:

C – Optical concentration [-]

$G_{concentrated}$ – Concentrated irradiance [W/m^2]

G_{1sun} –Non-concentrated irradiance [W/m^2]

$I_{sc,\ concentrated}$ – Short circuit current under concentrated irradiance [A]

$I_{sc,\ 1sun}$ – Short circuit current under non-concentrated irradiance [A]

Geometrical concentration can be calculated using the geometrical dimensions of the concentrator. Equation 7 can be used to calculate it:

$$C_G = \frac{A_c}{A_r} \tag{7}$$

Where:

C_G – Geometrical concentration [-]

A_c – Collector aperture area [m^2]

A_r – Receiver area [m^2]

Ideally, values of concentration calculated by Equations 6 and 7 should be equal. However, since real-life systems sometimes have imperfections which cause, that not all parallel light is directed to the focus, these values may differ. Equation 6 allows for an experimental determination of the concentration present in the system.

Due to high concentration levels, solar cells can heat up to extreme temperatures. Hence, a cooling system is necessary to reduce the temperature of the system and avoid damage.

Systems with lenses quite often use a passive cooling method. In such systems, a large plate is connected to the backside of the solar cells. The plate, which is often made of copper, has a high thermal conductivity, which allows the heat from the solar cell to be conducted to the plate. Because of a large surface area of the plate, the heat can be relatively easily dissipated into the surrounding air [22].

In the case of mirrors, such a large conducting plate cannot be integrated as easily, as it would block a large fraction of the light. Therefore, an active cooling system is usually used in such instances. For instance, a continuous flow of a coolant (such as water) along the backside of the cell can be used to actively cool the solar cell [22].

For the CPV systems, usually III-V solar cells are used. III-V PV technology utilizes elements of the 3rd and 5th groups of the periodic table. It is due to the fact that the III-V multijunction have the highest efficiency of all available solar cells and that efficiency of III-V solar cells is even higher under concentrated light conditions.

Generally, in the CPV systems the linear increase of the short circuit current and logarithmic increase of the open circuit voltage occur, which causes the electrical efficiency of a cell to increase. This pattern however is only present for light concentration up to 100 suns. At around a concentration of 100 suns and above, the efficiency of the solar cell starts to decrease significantly [22].

2.2.2 Concentrated solar power

Photovoltaic technology competes also with concentrated solar thermal power plants. Photovoltaic systems convert sunlight directly to electricity, whereas solar thermal power plants first convert sunlight to heat, and only then is the heat transformed into electricity. Such technology is commonly known as Concentrated Solar Power (CSP) and is more widely used than CPV.

CSP technologies use two general types of concentrators: linear focusing concentrators and point focusing concentrators. Within the former, two technologies can be distinguished: parabolic trough concentrators and systems using Fresnel lenses. Within the systems which concentrate solar radiation

into a point, one can distinguish two other technologies: solar towers and parabolic dish systems These systems tend to have much greater concentration factors. Some of these systems have a possibility of storing heat, which can later be transformed into electricity when there is demand for it. Others can operate as hybrid systems with fossil fuel or biomass combustion. Thus in total one can distinguish four main technologies, and they are as follows: parabolic troughs, linear Fresnel reflector systems, Parabolic dish systems and solar towers with molten salt heat storage [23].

A parabolic trough system consists of rows of curved mirrors to concentrate light on a line. The receiver is a pipe through which working fluid flows. Parabolic through plants operate commercially and they usually use synthetic oil as working fluid. The heat absorbed by the oil is then used to evaporate water which is then used to run a steam turbine. Parabolic troughs are the most mature technology out of all Concentrated Solar Power technologies [24]. Parabolic trough systems use one axis sun tracking. Figure 9 shows a parabolic trough collector:

Figure 9. Parabolic trough collector at Solar Platform of Almeria in Tabernas Spain [25]

Even though parabolic through systems usually have no heat storage, they can be equipped with a thermal storage system [24]. In the CSP technology, usually inorganic molten salts are used to store heat. Quite often it is a mixture of KNO3 and NaNO3 in 40%-60% ratio [24].

Linear Fresnel reflectors (LFR) focus light on a line and the receivers used in the system are fixed. Linear Fresnel reflectors use long rows of curved or flat mirrors and concentrated light on a linear receiver. The idea has recently been extended and a technology of compact linear Fresnel reflectors (CLFR) came to being. In such systems, two parallel receivers for each row of mirrors are used. This solution leads to decreasing the land needed to generate a given amount of energy compared to a parabolic trough system. LFR systems use one axis sun tracking [24].

There is a number of advantages of LFR systems with the main being lower investment costs due to their simplicity. They also facilitate direct steam generation – discussed later, thereby eliminating the necessity of heat exchangers and heat transfer fluid – further decreasing the cost of such systems.

The main drawback of LFR is their solar to electricity efficiency, which is lower than that of parabolic troughs. Moreover, incorporating storage capacity to these systems is more difficult [24].

Parabolic dishes focus light on a focal point which is located above the centre of the dish. These systems need to be equipped with a two axis solar tracker to make effective use of the solar radiation. Most parabolic dishes also have their independent generator. Usually a Stirling engine is used as a generator, however sometimes a micro-turbine is installed in the system. Given that, there is no need for any cooling system or heat transfer fluids in this design [24]. Figure 10 shows a group of parabolic dishes.

Figure 10. Parabolic dishes for heat generation in White Cliffs, Australia [20]

The concentration ratio in parabolic dishes is much higher than the one in parabolic troughs and can even exceed 2000 [23]. Due to the simplicity of the technology, the lack of cooling system, working fluid, etc. parabolic dishes can be cheap and cost-effective [23]. The technology however is not yet mature and more research is needed in this field. Yet, the advantages these systems show that parabolic dishes might have a bright future [24].

Solar tower with molten salt heat storage is a large-scale technology. First, heat is generated and stored and then it can be converted into electricity, whether or not the sun is shining. In a close vicinity to the tower, a set of mirrors, called heliostats, is located. These heliostats reflect sunlight to the receiver which is located at the top of the tower. In commercial systems the receiver is filled with molten salts, which absorb heat and reach temperatures of over 500°C. Afterwards, the molten salts are used to generate steam which then powers a steam turbine to generate electricity [26]. Apart from molten salts, other ways of energy storage are also being actively investigated. Solar tower installations use two axis solar tracking [26]. Figure 11 shows a solar tower installation.

Figure 11. Solar tower with molten salt heat storage near Seville, Spain [25]

In CPS systems, energy can be stored with various media. Most common ways of storing energy are the use of oils, the use of molten salts and direct steam generation. It is the latter that current research mainly focuses on and it has a great potential.

Direct steam generation (DSG) is a technology in which instead of a working fluid such as oil, water is used. Concentrated solar energy is directly used to evaporate water generating high-temperature steam. Water vapor is then used in steam turbines to generate electricity [27]. There is a number of ways that can be used to focus solar radiation for DSG – one can use mirrors or Fresnel collectors [27]. Troughs can also be used, and they were quite successful on a small scale – there are however significant difficulties that need to be overcome in order to scale this technology up [24]. Direct Steam Generation could significantly reduce the cost of investment and currently a lot of research is being conducted to further investigate the potential of this technology [24].

2.2.3. Simultaneous heat and electricity production

Sometimes however, Concentrated Solar Power technology is combined with Concentrated Photovoltaics in order to generate both heat and electricity simultaneously. An example of this technology is a Concentrating Photovoltaic Thermal (CPVT) system.

After the oil crisis in 1973 and 1974, scientists began to look for and develop alternative energy technologies – solar energy systems amongst others. First concepts of photovoltaic thermal collectors came to being in 1970ties, which were able to generate both heat and electricity with low efficiency [28]. The idea of combining photovoltaic systems with concentrators was first introduced in the 1970s and became an attractive field of research in early 1980s [29]. CPVT collectors are the last improved and efficient hybrid solar collectors, with the first CPVT collector having been constructed in 1977 at Sandia National Laboratories [30].

CPVT collectors usually use one or several curved mirrors to focus light onto the receiver. A schematic diagram of a CPVT collector is shown in Figure 12:

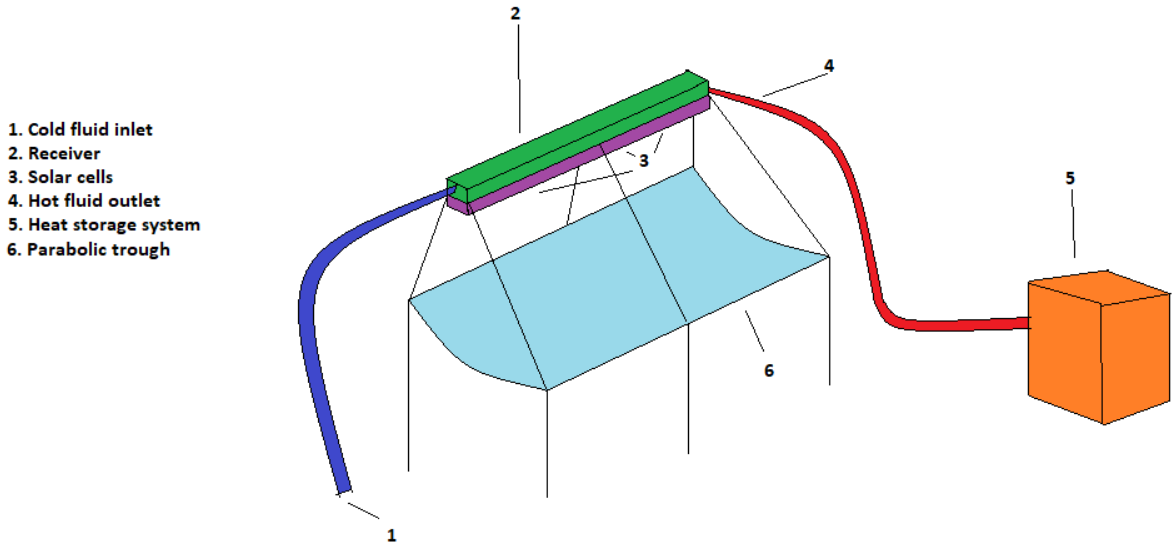

Figure 12. Schematic diagram of a CPVT collector

The receiver is equipped with solar cells, which under concentrated irradiance generate more electricity when compared to a conventional photovoltaic system of equal size. Working fluid flows through the receiver and absorbs heat from the walls thus generating useful heat. Working fluid also plays a role of a coolant, decreasing the temperatures of the solar cells.

CPVT is not a mature technology, thus CPVT collectors are not used commercially. The technology is currently being actively researched, and numerous prototype installations have been assembled. One such collector is shown in Figure 13:

Figure 13. Prototype CPVT collector in Athens, Greece [31]

Details regarding the processes of electricity and heat generation in Concentrated Photovoltaic Thermal collectors will be discussed in the next two subchapters.

2.3 CPVT electricity generation

In CPVT collectors electricity is generated by the solar cells attached to the receiver. However, due to the fact that concentrated sunlight is used in such systems, the type of cells and their chemistry is of paramount importance. Ideally, one would expect the cells to have high efficiency under these conditions, be cheap, have high resistance to thermal stress (high temperatures) and to conduct heat easily. Since fulfilling all these parameters is almost impossible, there is a number of cell types that could be used in CPVT systems depending on application.

The most popular materials for solar cells is crystalline silicon. These cells are often referred to as 1st generation solar cells. Currently, around 90% of all commercially available PV panels are based on the technology of either monocrystalline or polycrystalline silicon [11]. Monocrystalline cells tend to have higher efficiency compared to polycrystalline cells, however the production of the latter is cheaper and easier. The best research cells can achieve the efficiency of over 25% under laboratory conditions but typical crystalline cell efficiency is at around 15-20% [32]. Silicon as a material has numerous advantages, including abundance (it is the second most abundant element in Earth's crust), it is nontoxic and chemically stable [13].

However, there are significant drawbacks of silicon, which limit the use of crystalline silicon cells in concentrated solar systems. It has a low absorption coefficient and is very temperature-sensitive, which means its efficiency drops drastically with the increase of temperature. The output power of crystalline silicon solar cells drops by 0.4% for every 1˚C rise in temperature [13].

Given all the reasons listed above, silicon cells are not used often in commercial concentrated solar energy systems. Most of such systems have very high concentration ratios and the use of other types of solar cells proves more beneficial. However, crystalline silicon cells can be used in concentration systems with low concentration factors, due to their lower cost [33].

Another type of cells that can potentially be used in CPVT systems are thin-film cells, also known as 2nd generation cells. In this group one can distinguish cells made of amorphous silicon, CdTe, CIS and CIGS. These cells have important advantages over the 1st generation cells – the main one being an even lower cost of this technology [32]. Even though these cells have a lower efficiency than crystalline silicon cells, the material properties of the 2nd generation cells make their use in research prototype CPVT systems worth investigating. However, there are certain issues with these technologies. Although in recent years relatively high efficiencies were achieved, when compared to crystalline silicon the efficiency is usually lower, especially for amorphous silicon. Also, thin-film cells generally tend to have a high degradation rate. Because of these reasons, thin-film cells are not widely used in CPVT collectors.

Concentrated solar technology is still considered a niche application – however for the vast majority of highly efficient CPV and CPVT systems, III-V solar cells are used. III-V PV technology utilizes elements of the 3rd and 5th groups of the periodic table. One of the most common 3rd and 5th group materials used in this technology are gallium and arsenic respectively. Other combinations between aluminium, gallium, indium, phosphorous and arsenic are also used.

It is important to note, that out of the elements listed above, only aluminium and phosphorous are relatively abundant in nature. Other elements are rare and much less abundant than silicon, which leads to very high costs of materials. Additionally, processing methods of these elements are expensive. Moreover, arsenic is a toxic element, whose processing is not environmentally friendly.

Still, III-V solar cells outperform any other PV technology, obtaining very high efficiencies and despite their cost, find numerous uses in niche industries such as space applications and concentrated solar

technologies. Multi-junction solar cells with III-V elements can reach an efficiency of over 37% under 1 sun irradiance, and exceed 45% under concentrated sunlight [34].

Another crucial aspect of the electricity generation in CPVT collectors is the temperature of the solar cells. There is a direct relationship between the cells' temperature and electrical current as well as voltage. The higher the temperature, the higher the short circuit current and the lower the open circuit voltage [22]. However, since the relationship between temperature and voltage is much stronger than that of temperature and current, with increased temperature, cells generate less electrical power [16].

Certain elements of CPVT collectors can reach very high temperatures, depending on the concentration factor. Even under 1 sun irradiance solar cells can reach 85°C [16]. Thus, when concentrating mirrors or lenses are used, high temperature can potentially damage cells and other pieces of equipment.

With this in mind, CPVT collectors use a cooling system. Its main purpose is to generate useful heat and it will be described in detail in the next subchapter. However, there is an additional purpose for the working fluid flow – it decreases solar cells' temperature. All efforts should be made to ensure effective heat recovery. That way more heat can be generated, and the cell's temperature would decrease more to enable higher electrical efficiency.

It is said that modern efficient CPVT collectors should achieve the electrical efficiency of at least 30%. This is the case for systems using the most efficient solar cells, mainly III-V solar cells [33]. However, due to Shockley-Queisser limit, theoretical maximum efficiency ,the maximum efficiency that could be achieved by a p-n junction PV cell with 1.1eV band gap is 33% [33]. In order to obtain higher efficiencies, multijunctions can be used and for such systems efficiencies of over 40% can be reached [33].

Early CPVT prototypes however obtained relatively low electrical efficiencies. Water-cooled CPVT system using monocrystalline silicon cells achieved electrical efficiency of 11% [31]. This parabolic trough system was designed by J.S. Coventry and its optical concentration was 37. Monocrystalline silicon cells were attached to an aluminum duct, which was colled with water at mass flow rates in the range of 37.5-42.5 mililiters per second [31].

Another early CPVT system which used a parabolic reflector and GaAs cells obtained 8,9% electrical efficiency [31]. This system was designed by M. Li et al and its concentration ratio was 31. The cooling system in this installation operated similarly to the one designed by Coventry.

Yongfeng et al investigated a similar system with GaAs cells with a concentration ratio of 10. The electrical efficiency of the system was 9.5% [31].

Vivar designed a CPVT installation with a Fresnel reflector. Its concentration ratio was equal to 20. In this system, two arrays of Fresnel reflectors were installed and they concentrated irradiance on two micro-receivers. These receivers were equipped with silicon solar cells, whose efficiency was equal to 8% [31].

Modern systems tend to obtain slightly higher electrical efficiencies. It has mainly to do with the advancements in the photovoltaics technology made in recent years. Araki et al investigated a CPVT collector which used Fresnel lenses and its electrical efficiency was as high as 25.8% [33].

2.4 CPVT heat generation

There are three mechanisms of heat transfer and they are as follows: conduction, convection and radiation. All of them are present in everyday life and essential to ensure operation of any solar heating system, including CPVT collectors.

Conduction is a molecular transfer of heat in a medium due to a non-uniform temperature distribution. Convection is a transfer of heat in a medium with an inhomogeneous temperature distribution, carried out by macroscopic elements of the medium during their movement. Whereas thermal radiation is a process of heat propagation by electromagnetic waves. This type of heat transfer is due to the transformation of internal energy of matter into radiation energy, transmission of the energy and its absorption [35].

In Concentrated Photovoltaic systems usually over 50% of the radiation energy is lost by being transformed into waste heat [36]. CPVT systems can make use of that heat and convert more radiation energy into a useful form.

When comparing CPVT and PVT collectors, one major disadvantage of the latter comes to mind: due to a relatively low temperature increase, thermal energy of such systems find its use in low-temperature applications only. In CPVT systems this problem is overcome, since the presence of concentrators can lead to a much greater temperature increase [33]. Still, it is important to note that there are low-concentration CPVT systems, which generate heat only for low-temperatures despite the use of mirrors or lenses. In those cases, the concentration ratios are much lower.

A thermal collector is a critical part of a CPVT system, which is responsible for heat generation. Parabolic troughs and dishes are the most commonly used concentrators in CPVT systems and flat plate absorbers can be used in such systems [29]. In CPVT systems with flat plate absorbers, a glass cover is used in order to minimize heat losses [29].

Parabolic troughs and dishes are used to concentrate solar beams, which are then reflected into PV cells. The cells heat up to high temperatures and a cooling system recovers heat from the back of the cells, which otherwise would be lost.

In case of a CPVT system with a parabolic trough, the principle of operation is very similar to a parabolic trough CSP system. The only difference is that in the former, PV cells are attached to the receiver and the heat is recovered from the back of them.

Synthetic oil can be used as working fluid in such systems, usually the ones with high concentration ratios. For low-concentrating photovoltaic thermal systems water can also be used. For high concentration systems high-temperature heat is generated, which can be used in a variety of applications. Low-concentrating systems generate low-temperature heat, which has limited uses [37].

Early CPVT prototypes obtained relatively low thermal efficiencies. Chaabane et al designed a linear CPVT system with a compound parabolic reflector. Its maximum thermal efficiency was as low as 16%. The receiver consisted of a rectangular duct equipped with monocrystalline silicon solar cells [31].

Du et al evaluated the performance of a CPVT system using linear Fresnel reflector with concentration of 8. The receiver was a U-shaped tube with silicon solar cells attached. System thermal efficiency was equal to 39% [31].

Li et al designed a prototype linear CPVT system with GaAs cells, and its thermal efficiency was equal to 41.7%. System's concentration ratio was 31 and it was cooled with water. The water flew through the aluminum duct to which GaAs cells were attached [31].

Modern efficient CPVT have high thermal and electrical efficiencies. The overall efficiency of such systems often exceeds 65% [33]. Prototype CPVT collectors with monocrystalline solar cells were reported to achieve thermal efficiency as high as 58% [31]. Other systems, using GaAs cells reached thermal efficiencies of 35-42% [31].

3. System design, construction and instrumentation

3.1 System Design and instrumentation

The objective was to design a prototype CPVT collector with a decent efficiency. In order to design the installation properly, all crucial aspects had to be taken into account. Beginning with a choice of the location, through the identification of all system components up to size and material specifications of each element.

The first decision that had to be made concerned the location of the installation. Due to the uncertain pandemic situation and the fact that the preparation of the installation should start as soon as possible, it was decided that it would be built in Cracow, Poland. The collector would end up being installed at the roof of the D9 building at the AGH Campus.

Then, the date of the measurements had to be agreed upon. Since Cracow, Poland does not experience as much solar irradiance as Lisbon, Portugal, it was crucial to complete all measurements in the summer months, when the expected irradiance would be the highest. Hence all elements of the installation had to be prepared and operational before the end of summer. Eventually, the measurements were conducted in July and August of 2021.

The next step in the designing process was to identify all necessary elements of the system. These could be divided into two separate groups: system components which are essential to ensure the system is operational, and additional elements which are of vital importance when performing measurements.

Key elements of the system are as follows: parabolic trough concentrator, heat absorbing duct, hosepipes and water source, sets of PV cells, Sun tracker, electronic load. In order to perform all necessary measurements, the following elements are needed: Multimeters, electronic load, IR camera, laser pyrometer, thermocouples, flow-meters, computer-supported measuring system.

The parabolic trough concentrator was designed to be 2m long. It consisted of curved polycarbonate construction and with reflecting mirrors attached with stripes. The concentrator was profiled based on computer simulations using TracePRO software.

Using software calculations as well as Equation 7 it was determined that the concentration would be equal to 4. Given that, it is expected that a low-concentrating photovoltaic thermal installation would be obtained. Figure 14 shows the dimensions of the concentrator.

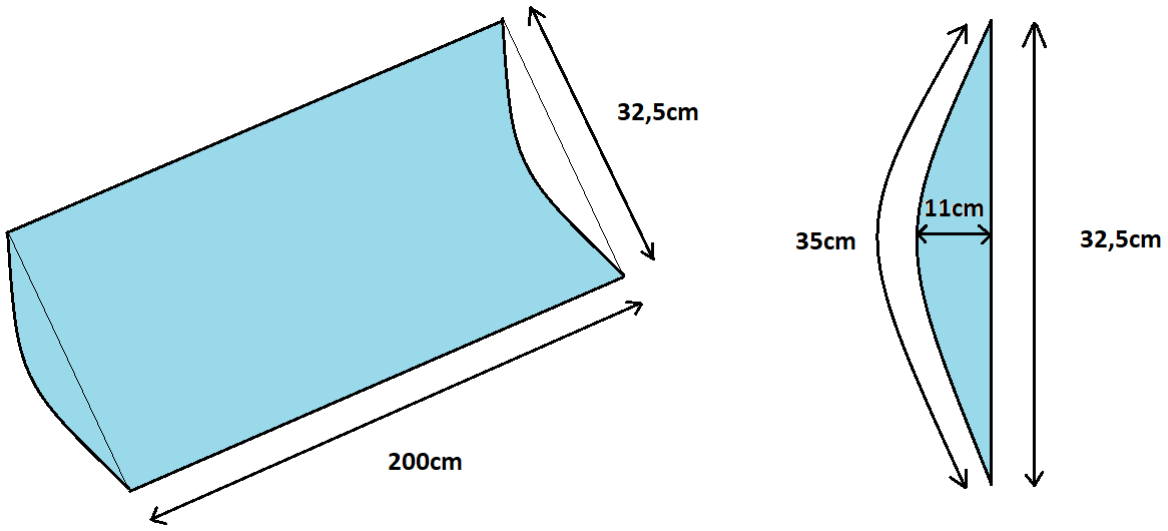

Figure 14. Concentrator dimensions schematic diagram

The heat absorbing duct was designed to be made of aluminum and in a hexagonal shape. The fluid flowing through the duct absorbs the heat and thus the temperature of the fluid rises. The hexagonal shape was chosen to make the system more flexible and allow for measurement of various parameters for a number of PV technologies at the same time, since 6 walls are available. The duct was also designed to be 2m long to fit with the concentrator. Figure 15 shows the schematic diagram of the duct.

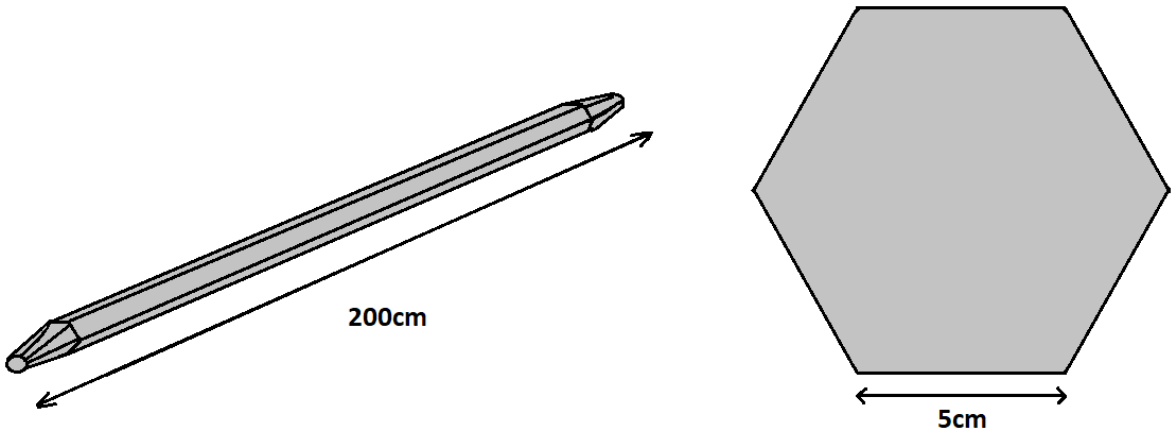

Figure 15. Heat-absorbing duct schematic diagram

Hosepipes were designed to fit the duct and allow for uninterrupted fluid flow. Initially a separate tank with the working fluid was being considered. However, since it was decided that water will be used as working fluid, for simplicity water was directed to the installation from the plumbing system.

The most important element of the system, that required vast amounts of preparation was the set of photovoltaic cells. First, the types of solar cells technologies to be used had to be chosen. Since the chemistry of the cells is of significant importance to the thesis, it was decided that high efficiency monocrystalline cells as well as amorphous silicon cells would be used. Since the concentration ratio in the system will be low, silicon-based solar cells would not be damaged. Cells would be connected in series and parallel and attached to the aluminum duct.

Electronic load is a device which absorbs the electrical power generated by a power source. In this case it absorbs the electrical power generated by the sets of solar cells attached to the aluminum duct. This particular load was also used as a measuring device, since some electrical parameters such as current and voltage could be read from the screen of the load. Electronic load Array ELD3711A [38] was used. The load was used to collect data on current, voltage and power for all cells connections and their operation under various conditions.

Two Fluke 179 TRMS [39] multimeters were used with DC voltage accuracy of ±(0.09% +2) and DC current accuracy of ±(1.0% + 3). They were only used to determine, whether individual cells operate properly and give expected output values under given conditions.

The following model of an infra-red camera was used: NEC ThermoTracer H2640 [40]. It was used to generate thermal images of the installations, which allowed for a detailed temperature analysis. Radiometric Thermography software was used to analyze the images obtained by the camera.

Laser pyrometer HP-880EK [41] was used in the measurements. It was used to determine the temperature of individual points of solar cells under various conditions.

An ambient air thermometer was used to measure the air temperature during the measurements.

Pt 100 thermocouples type K [42] were used in the measurement process. They were used to determine water temperatures on the inlet and on the outlet of the system, when water flew through the receiver.

Benning Sun 2 pyranometer [43] was used to measure the irradiance. It was used to determine the amount of irradiance reaching the solar cells under non-concentrated irradiance conditions.

GMDM –I model of a water flow meter [44] was used. It was used to determine the water flow of the coolant flowing through the receiver.

Computer was connected to the system, and using CodeSys software [45] it was possible to collect data regarding inlet and outlet temperature and export them as a database.

Details on how measuring equipment was used and what parameters were measured will be shared in the experimental analysis chapter.

3.2 System Construction

A steel construction with a two-axis solar tracker was installed at the rooftop of a D9 building at the AGH campus in Cracow. It was set up in the centre of the rooftop in order to ensure that no trees, buildings or other installations on the roof would block out any part of the installation. The structure was equipped with elements which would allow for an easy connection of the aluminum duct.

The concentrator was constructed by attaching a flexible mirror to the surface with glue. The reflectivity of the mirror used was 85% in the spectrum of visible light. The mirror was carefully attached and all measures were taken to make sure the reflective surface would be smooth. However, some parts were not perfectly smooth, which potentially can lead to some optical errors with concentration.

The concentrator was placed onto the construction in a proper way in order to ensure that the light will be concentrated into a focus, right where the receiver will be installed. Figure 16 shows how the installation looked at this point.

Figure 16. Concentrating mirror

The next step was to prepare the heat-absorbing duct. Aluminum hexagonal shape duct had to be equipped with photovoltaic cells in a proper way to ensure effective heat transfer from the cells to the working fluid.

The preparation of this part of the system began with connecting the PV cells in sets. Initially, thin-film amorphous silicon cells were connected in series in sets of 3 cells each. Analogically, monocrystalline silicon cells were connected. This design would ensure more flexibility and allow for various types of connections to be investigated in the experimental part of the project.

Individual cells were soldered and connected to one another via copper wires. Wires were equipped with insulation to make sure no short-circuit would appear. Malfunctions like this could damage the cells permanently. Before proceeding, multimeters were used to check whether the connections are functional and the cells remain operational. Figure 17 presents the thin-film cells connecter in series.

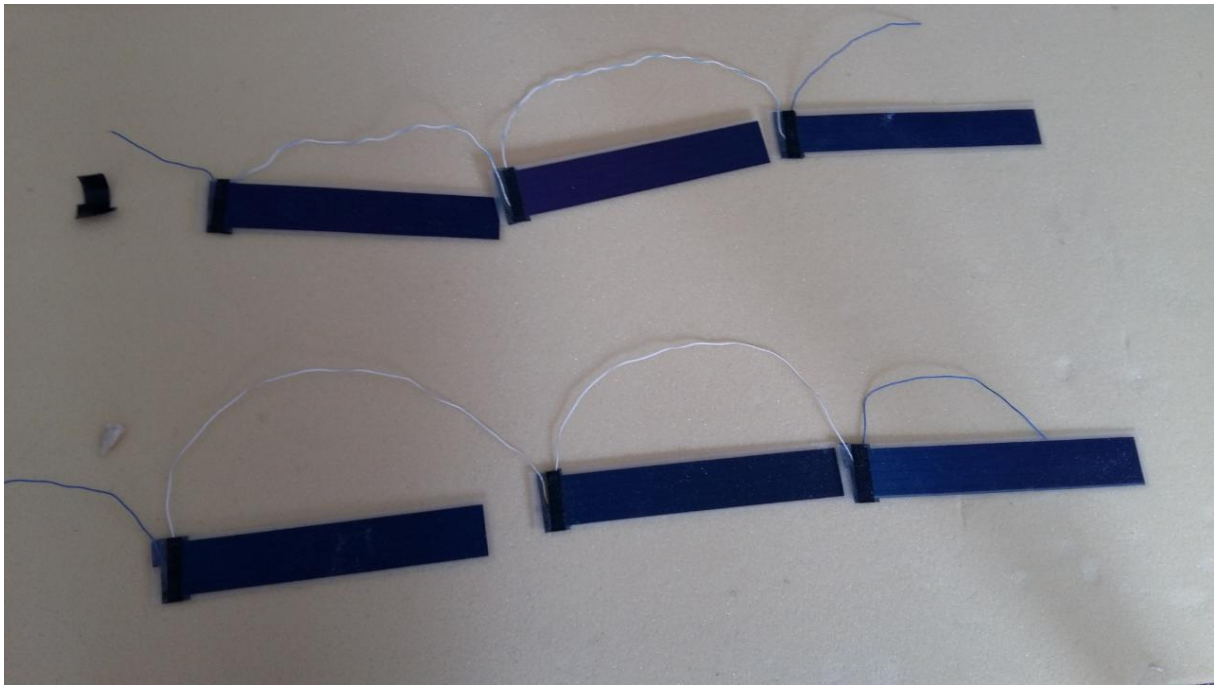

Figure 17. Amorphous silicon cells connected in series

In total, 9 thin-film amorphous silicon, as well as 12 monocrystalline silicon cells were used for this project. The numbers were chosen due to the dimensions of each cell – to make sure the total length of the cells does not exceed the length of the duct. Furthermore, those numbers allow more flexibility when choosing the final types of connections when performing the analysis.

Once the cells were soldered and connected, they had to be attached to the aluminum duct. It was decided that thermally conductive adhesive AG TermoGlue would be used to attach the cells to the receiver.

A thin layer of the thermally conductive adhesive was put on two the walls of the duct. Just enough glue was used to make sure the cells would not come away. Too much adhesive could decrease thermal conductivity. One wall was equipped with 12 monocrystalline silicon cells, whereas 9 thin-film amorphous silicon cells were attached to the second one.

Since in the frames of the thesis only two technologies of solar cells (monocrystalline silicon and amorphous silicon) are being investigated – it was decided to attach cells only to two walls. The space on other walls allowed for more flexibility when transporting the duct. The duct can be thus easily placed on any surface for the purpose of measurements on empty sides without the fear that cells could get damaged due to mechanical stress. Furthermore, free space on other walls can later be used for future work.

Cells were carefully pressed to the walls so as not to damage them and the wires. Once attached, the cells were left for 24 hours until the glue has dried. After 24 hours cell connections were checked once again, and they were functioning properly. Hosepipes were attached to both ends of the aluminum duct to check whether there are any issues with the water flow. No issues were detected up to this point. Some measurements were already made at this point to understand how much energy could be harnessed by the system under 1-sun irradiance. Figure 18 shows the heat absorbing duct with attached PV cells connected to the water system via hosepipes:

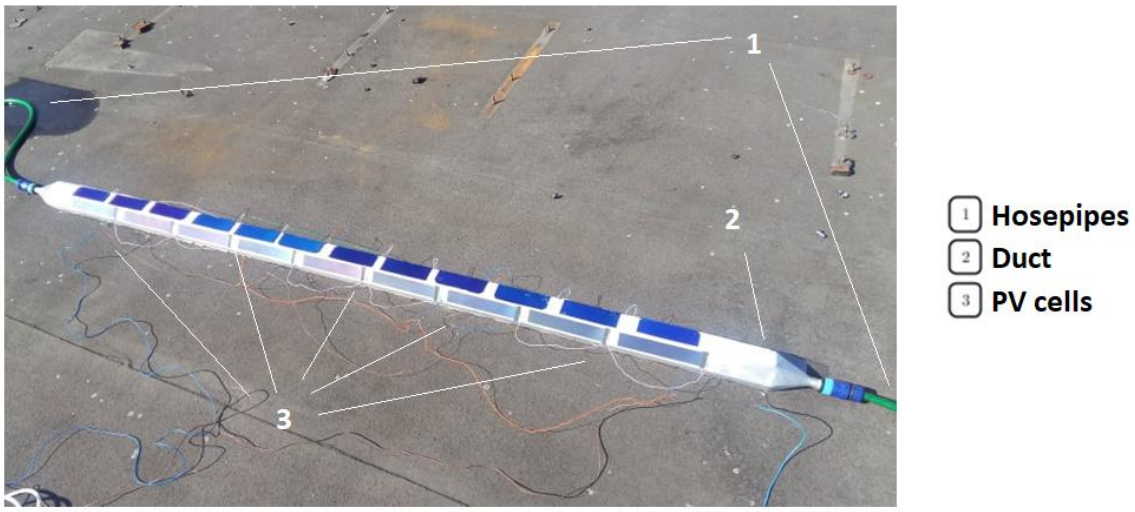

Figure 18. Receiver equipped with solar cells

Since everything was working properly, the duct with solar cells was ready to be installed above the concentrator. Having placed the concentrator, all connections were checked once again. No malfunctions were detected, thus the installation was ready for measurements. Figure 19 shows a fully assembled prototype CPVT installation:

Figure 19. Fully assembled CPVT installation

All information regarding the collected data and performed measurements, as well as the use of measuring devices will be described in the next chapter on experimental analysis.

4. Experimental analysis, results and discussion

4.1 Experimental methodology

The main methodologies will be presented in this chapter. The goal of the thesis is to build a CPVT installation, gather necessary data and evaluate the performance of the installation.

In order to evaluate the operation of the installation, quantitative data of electrical and thermal parameters were necessary. So as to compare the performance of this installation to other, existing ones – results obtained in this analysis were compared with. These data included electrical and thermal efficiency values, among many other.

In order to measure the parameters, several instruments were used. In the case of electrical parameters, values of voltage and current were collected using multimeters and an electronic load. Solar cells were connected to the load via wires, and the values were read from the load's screen. The electronic load showed values of current, voltage and power, and these values were collected and analyzed.

In the case of thermal parameters, the measurement of the temperature was of vital importance to the thesis. Temperature of solar cells were measured using two instruments – a laser pyrometer and an Infra Red camera. The pyrometer allowed for the determination of temperature of individual points, while the IR camera generated whole thermograms showing key elements. Water temperature was measured with thermocouples.

First, electrical parameters of individual cell were measured under a clear sky and the irradiance of 850±25 W/m^2 to ensure that they operate properly and no malfunctions were detected. Then, the cells were connected in groups, and the electrical parameters of groups of cells were measured under the same conditions to ensure that the connections were made properly.

Then, complete final connections described in the following chapter were made and the cells performance was measured under both non-concentrated and concentrated irradiance without cooling. The cells were properly oriented to the sun with the help of a sun tracker in each case, thus all measurements were conducted under the same conditions.

Then, the thermal parameters of the system were measured. Air temperature was being measured near the installation throughout the whole process of measurement. The temperature of individual cells in key points was measured with a pyrometer at the conditions of both non-concentrated and concentrated irradiance. For the cells under non-concentrated irradiance, an IR camera was used to generate thermal images of the cells. The temperature of the cooling water flowing though the system was measured with thermocouples.

Finally, thermal and electrical parameters were measured for the system when cooling was used. These results were then compared and described.

In order to improve accuracy of collected data, each measurement was repeated three times. All electrical parameters were noted down and analyzed with the Excel software. Excel was also used to prepare charts and tables. For thermal part analysis in addition to Excel, Radiometric software was used for IR camera images analysis.

4.2 Solar cells electrical parameters analysis

Before attaching the solar cells onto the receiver it was necessary to make sure all cells were working properly. For this purpose, individual cells were checked using a multimeter.

The multimeter readings showed the values of open circuit voltage that are achieved under given conditions. All cells were tested this way under the irradiance of around 850±25 W/m^2 , that is the conditions under which the final installation would operate. The voltage values were then compared to the values given at a specification sheet for the cells. Since, apart from one thin-film cell, no major differences were noticed, it was assumed that the cell operate properly and can be used in further stages of the project.

Once the cells were connected in sets in series, the same procedure was applied. No malfunctions were detected. After attaching the cells to the receiver, completing cells connections and adding an electronic load to the system, the measurement of electrical parameters could begin.

First, cells connection under 1-sun irradiance were analyzed. Three groups of three thin-film cells connected in series were investigated first – each group was analyzed individually. Then, these three sets were connected in parallel and electrical parameters of such a connection were measured. The measurements were performed under the clear sky, with the irradiance of 850±25 W/m^2 and a proper orientation towards the sun. Taking into account the relationship between voltage and current of parallel and series connections, as well as the specifications of the thin-film cells, it was decided that such a connection would deliver the most meaningful results, due to suitable ranges of voltage and current obtained. Figure 20 shows how the thin film amorphous silicon cells were connected. They will be referred to as Set A (a-si) in further parts of the thesis.

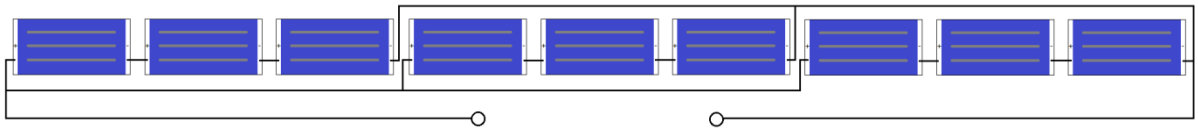

Figure 20. Set A (a-si) connection schematic diagram

Then monocrystalline silicon cells were analyzed, with first focusing on four groups of three cells connected in series – each group was analyzed individually. Then, all twelve cells were connected in series and their electrical parameters were measured. Taking into account the relationship between voltage and current of series connections, as well as the specifications of the monocrystalline silicon cells, it was decided that such a connection would deliver the most meaningful results. Figure 21 shows how the monocrystalline silicon cells were connected. They will be referred to as Set B (m-si) in further parts of the thesis.

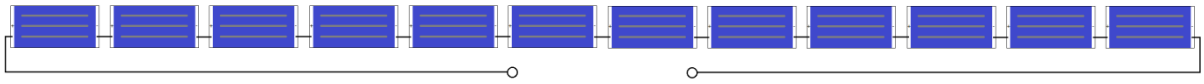

Figure 21. Set B (m-si) schematic diagram

All measurements in this section were repeated three times to ensure the results are valid. Since no major differences between the results were detected, the average values were calculated and presented in figures.

The distribution of each group of amorphous silicon cells is shown in Figure 22:

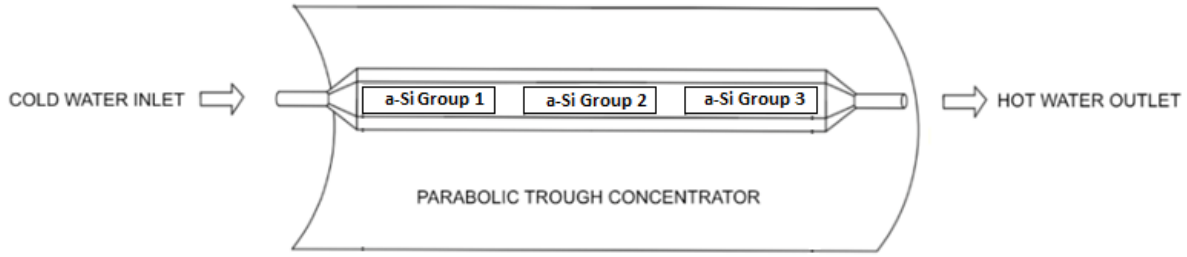

Figure 22. Schematic diagram presenting the location of each group of a-Si cells

The distribution of each group of monocrystalline silicon cells is shown in Figure 23:

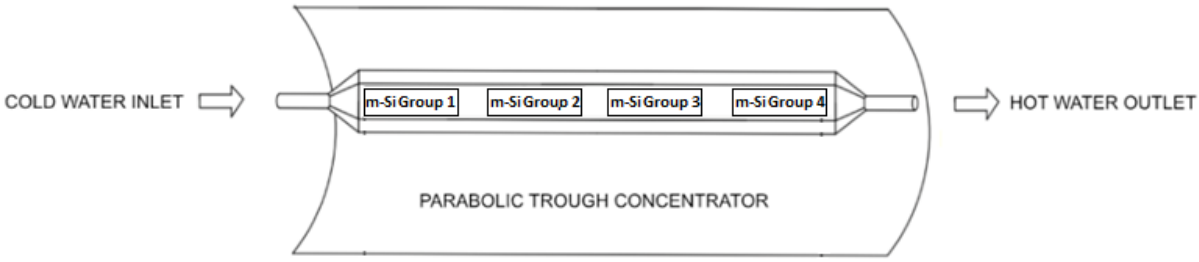

Figure 23. Schematic diagram presenting the location of each group of m-Si cells

All measurements were performed under a clear sky. The irradiance ranged from around 825 W/m^2 to around 875 W/m^2 during the measurements. It was thus assumed, that the average irradiance was equal to 850±25 W/m^2, and this value will be used in further calculations.

Figure 24 shows the data points and the I-V curves for the groups of three thin-film cells connected in series.

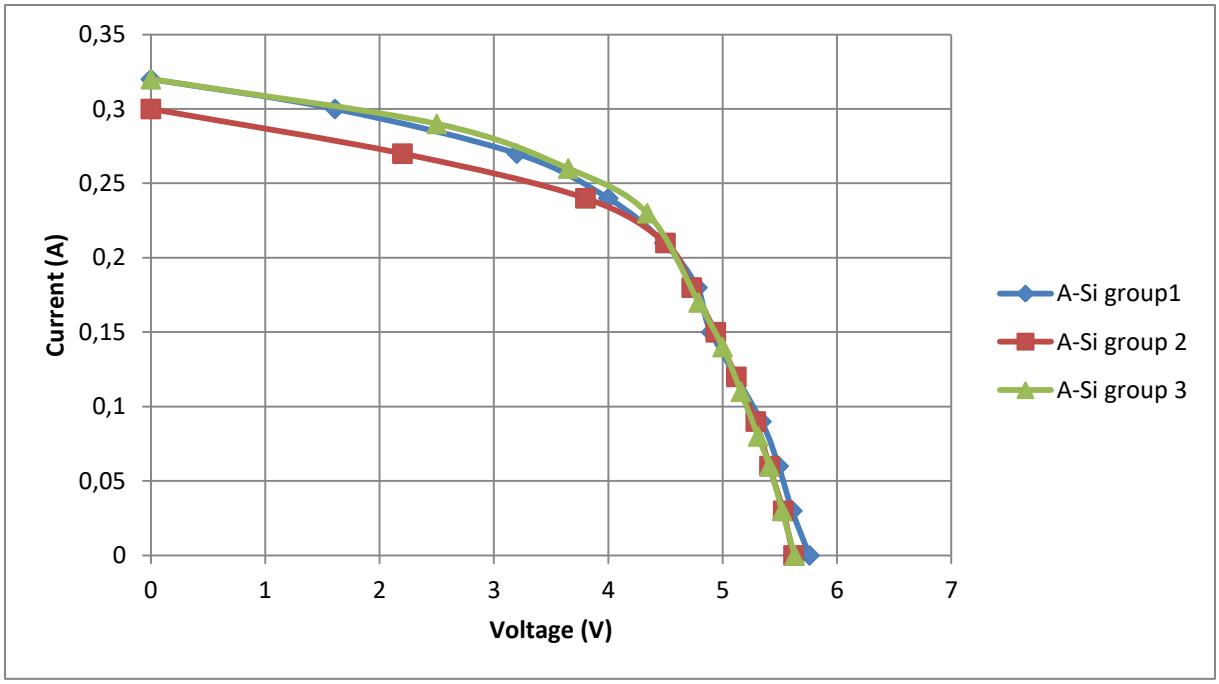

Figure 24. I-V curves for the groups of three thin-film cells connected in series

The average short circuit current for these groups is 0,31± 0,01 A and the average open circuit is equal to 5,67± 0,01 V.

Figure 25 shows the data points and the power curves for the groups of three thin-film cells connected in series.

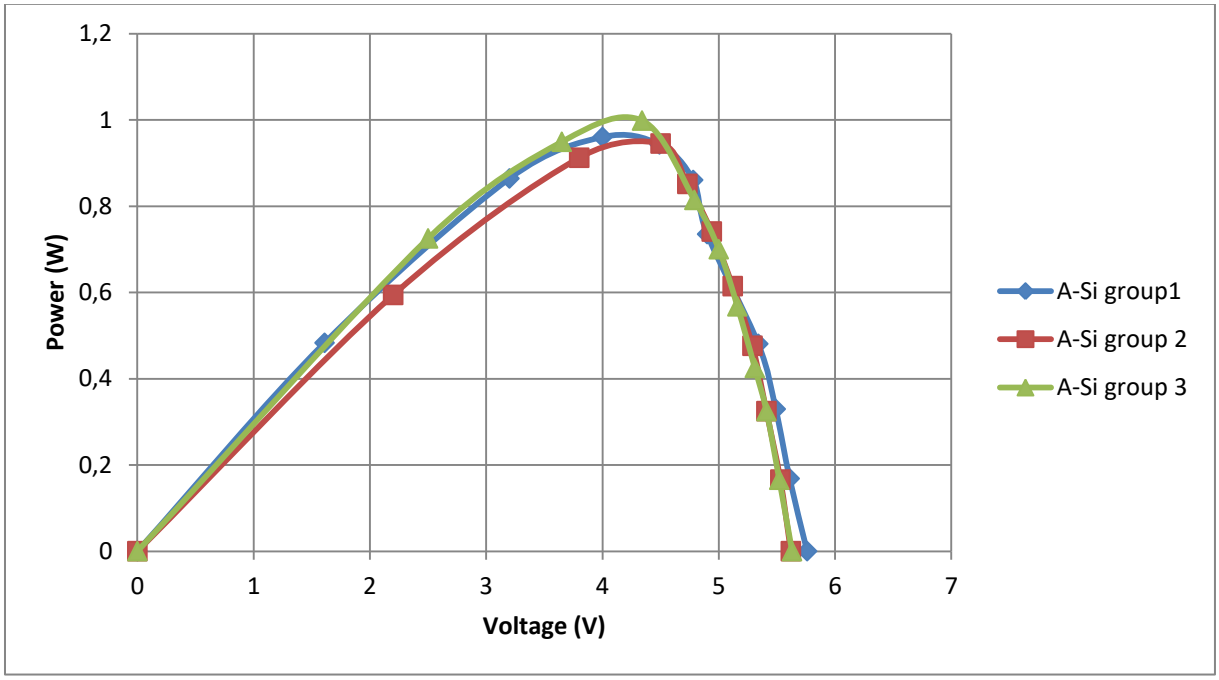

Figure 25. Power curves for the groups of three thin-film cells connected in series

The average maximum power generated by these groups of cells is equal to 0,97± 0,01 W.

Figure 26 shows the data points and the I-V curve for Set A (a-si):

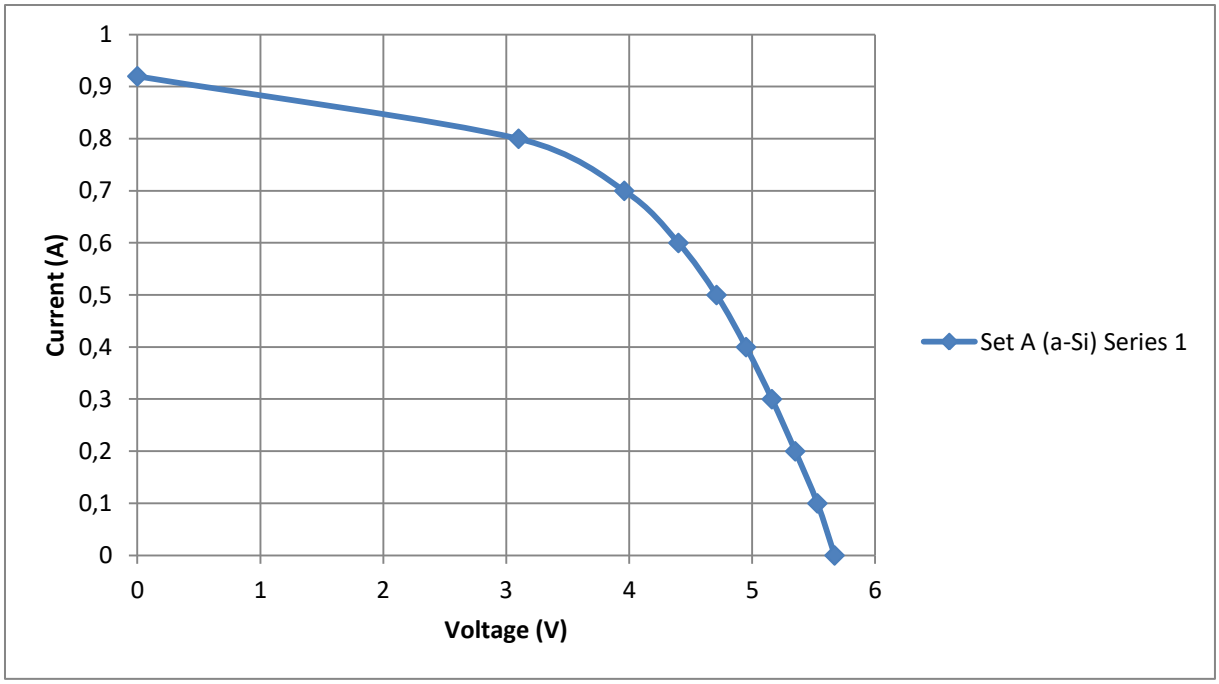

Figure 26. I-V curve for Set A (a-Si)

The values shown in Figure 26 are calculated as the average of three measurements. The short circuit current is 0,92 ± 0,01 A and the open circuit is equal to 5,67 ± 0,01 V.

Figure 27 shows the data points and the power curve for Set A (a-si):

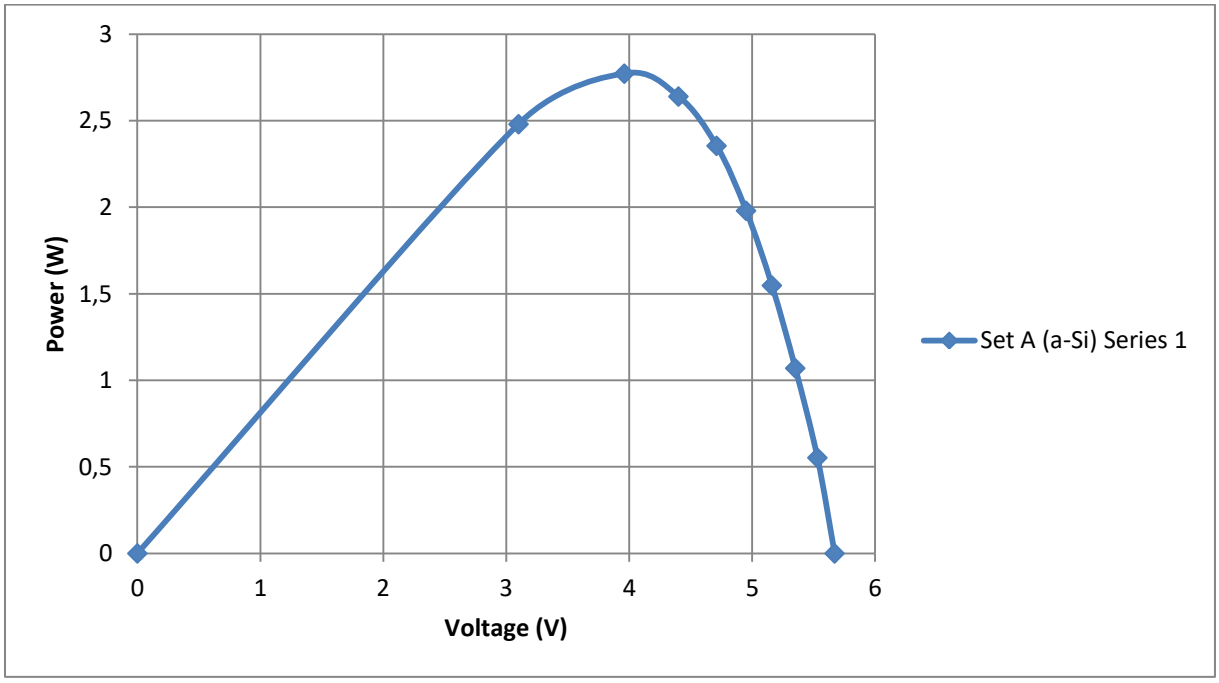

Figure 27. Power curve for the Set A (a-si)

The maximum power generated by these cells is equal to 2,77 ± 0,01 W.

When comparing the data points for groups of 3 cells connected in series, to the case where these 3 groups were connected in parallel one can notice that the short circuit current is approximately three times larger in the latter case, while the open circuit voltage remains the same. These results are

expected, since connecting the same cells or group of cells in parallel increases the I_{sc} – short circuit current, but does not alter the V_{oc} – open circuit voltage. This once again proves that the connections were prepared correctly and the cells operate as expected.

Equation 2 was used to determine the electrical efficiency of Set A (a-si). The total area of all 9 a-Si cells is equal to 0,04725 m^2 and solar irradiance was assumed to be 850±25 W/m^2 and the maximum power generated is equal to 2,77±0,01 W. The electrical efficiency of Set A (a-si) is equal to 6,90±0,12%.

Figure 28 shows the data points and the I-V curves for the groups of three monocrystalline silicon cells connected in series:

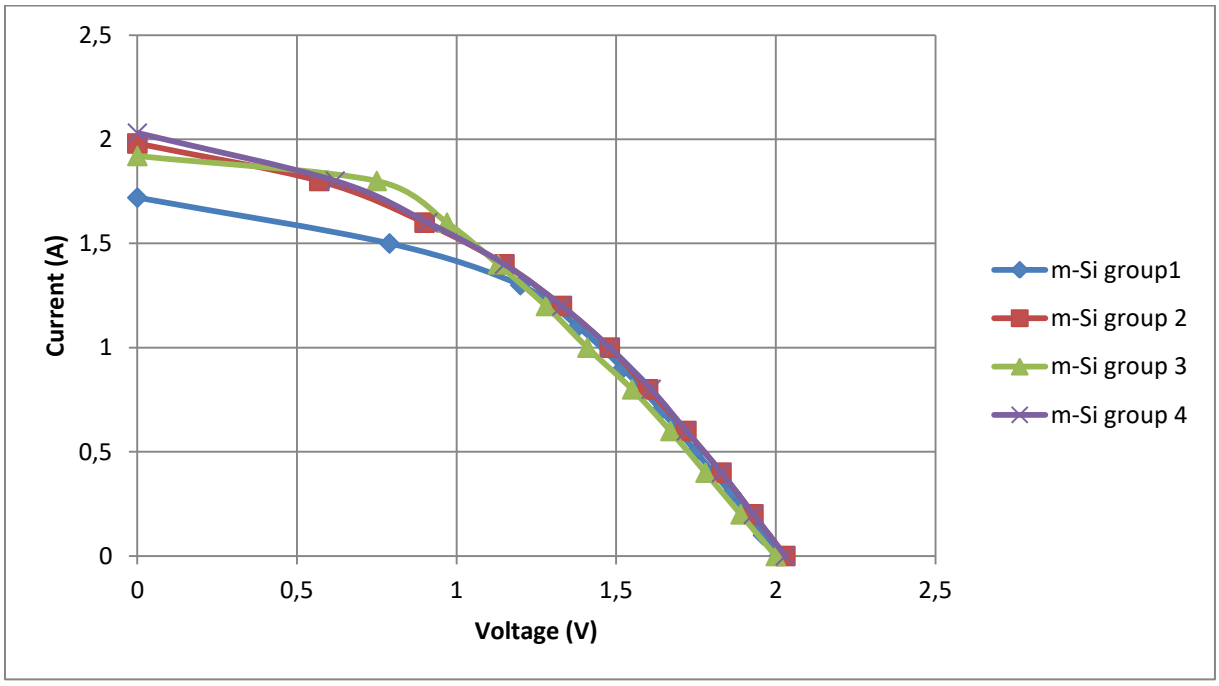

Figure 28. I-V curves for the groups of three monocrystalline silicon cells connected in series

The average short circuit current for these groups is 1,91± 0,01 A and the average open circuit is equal to 2,02± 0,01 V.

Figure 29 shows the data points and the power curves for the groups of three monocrystalline silicon cells connected in series:

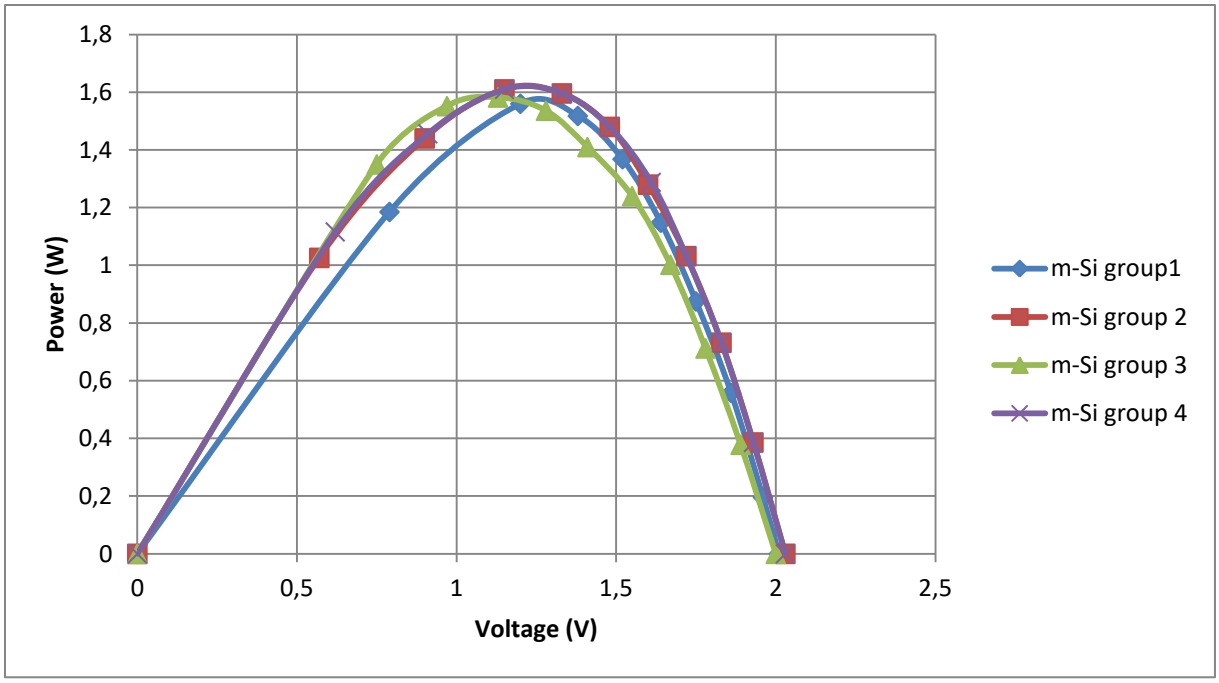

Figure 29. Power curves for the groups of three monocrystalline silicon cells connected in series

The average maximum power generated by these groups of cells is equal to 1,59±0,01 W.

Figure 30 shows the data points and the I-V curve for Set B (m-si):

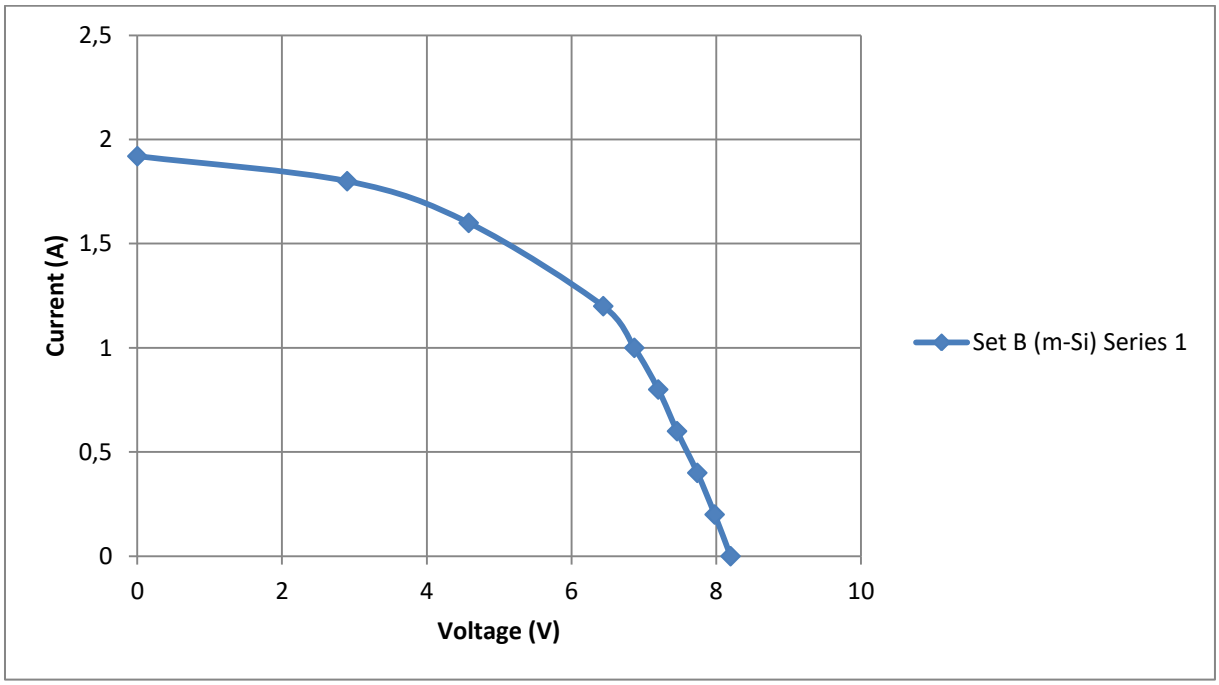

Figure 30. I-V curve for Set B (m-si)

The short circuit current is 1,89±0,01 A and the open circuit is equal to 8,18±0,01 V.

Figure 31 shows the data points and the power curves for Set B (m-si):

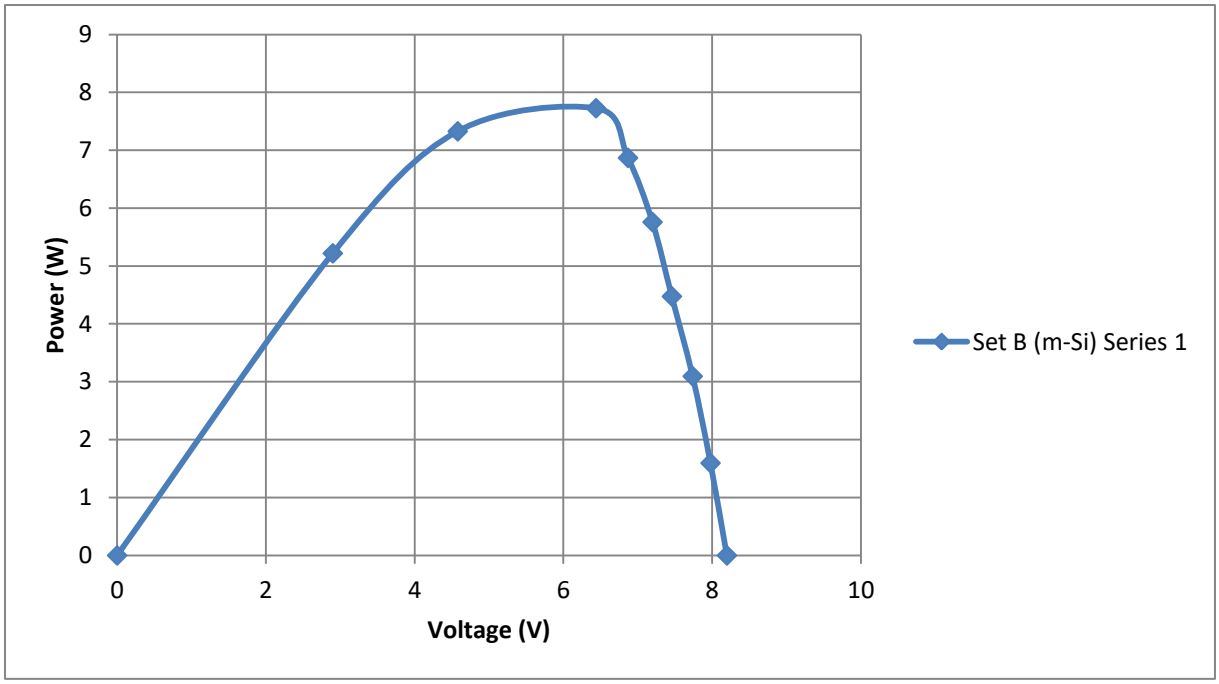

Figure 31. Power curve for Set B (m-si)

The maximum power generated by these cells is equal to 7,91± 0,01 W.

When comparing the data points for groups of 3 cells connected in series, to the case where all 12 cells were connected in series one can notice that the short circuit current remains the same, while the open circuit voltage increased four times. These results are expected, since connecting the same cells or group of cells in series increases V_{oc}, but does not alter the I_{sc}. This once again proves the connections were prepared properly and the cells operate as expected.

Formula 2 can be used to determine the electrical efficiency of Set B (m-si) as well. Given that the total area of all 12 m-Si cells is equal to 0,0624 m^2 and solar irradiance was equal to 850±25 W/m^2 and the maximum power generated is equal to 7,91±0,01 W, the maximum electrical efficiency of monocrystalline silicon connected in the above-mentioned way is equal to 14,91±0,25%.

Set A (a-si) and Set B (m-si) were then investigated under concentrated irradiance too. They were placed above the concentrator and their electrical parameters were measured, so as to create I-V curves for such conditions.

Figure 32 shows the data points and the I-V curve for Set A (a-si) under concentrated irradiance:

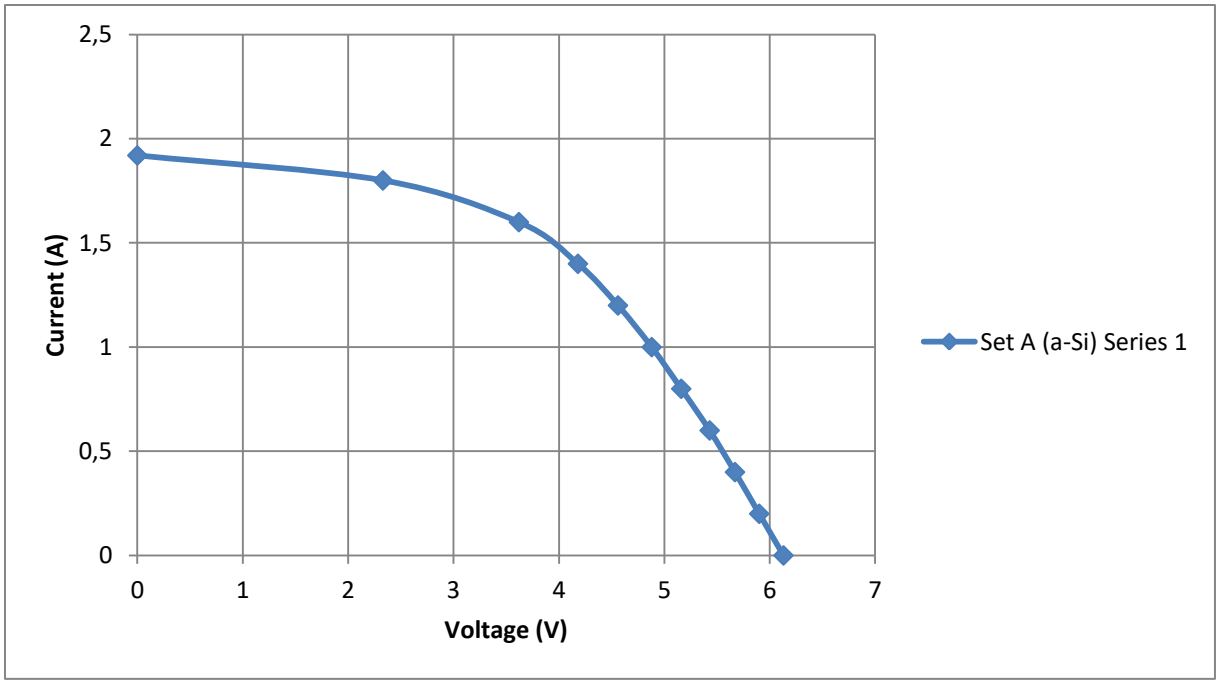

Figure 32. I-V curve for Set A (a-si) under concentrated irradiance

The short circuit current is 1,93± 0,01 A and the open circuit is equal to 6,1± 0,01 V.

Figure 33 shows the data points and the power curve for Set A (a-si) under concentrated irradiance:

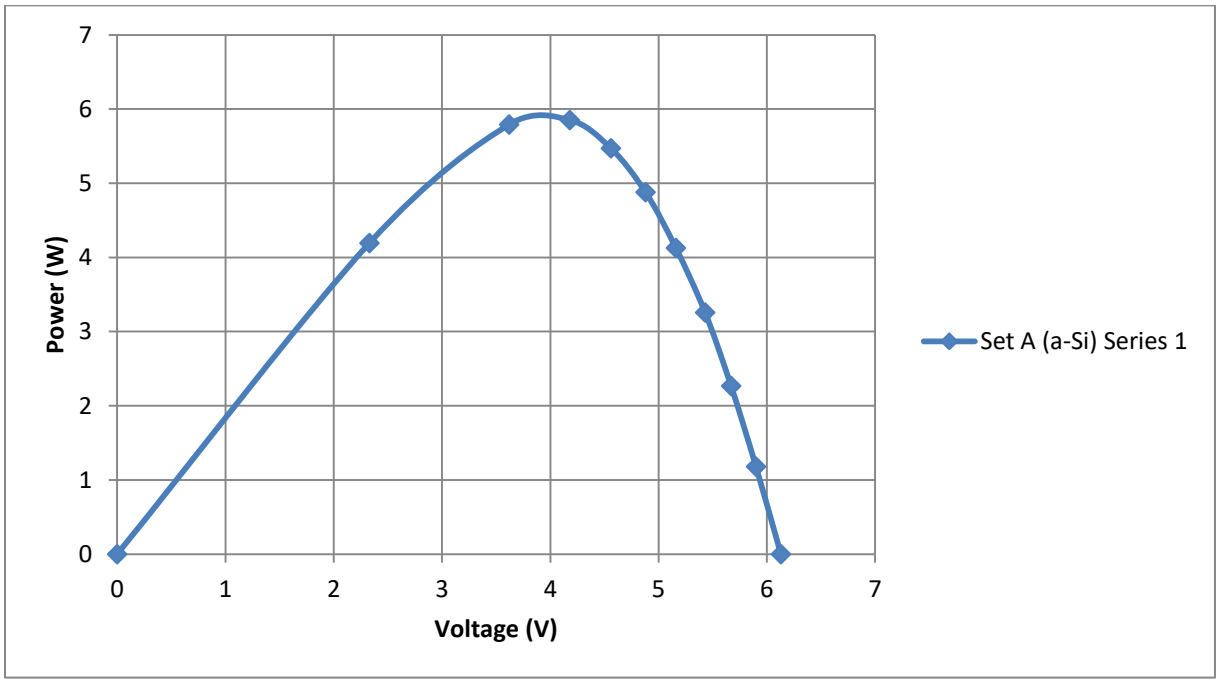

Figure 33. Power curve for Set A (a-si) under concentrated irradiance

The maximum power generated by these cells is equal to 5,98± 0,01 W.

Figure 34 shows the data points and the I-V curves for Set B (m-si) under concentrated irradiance:

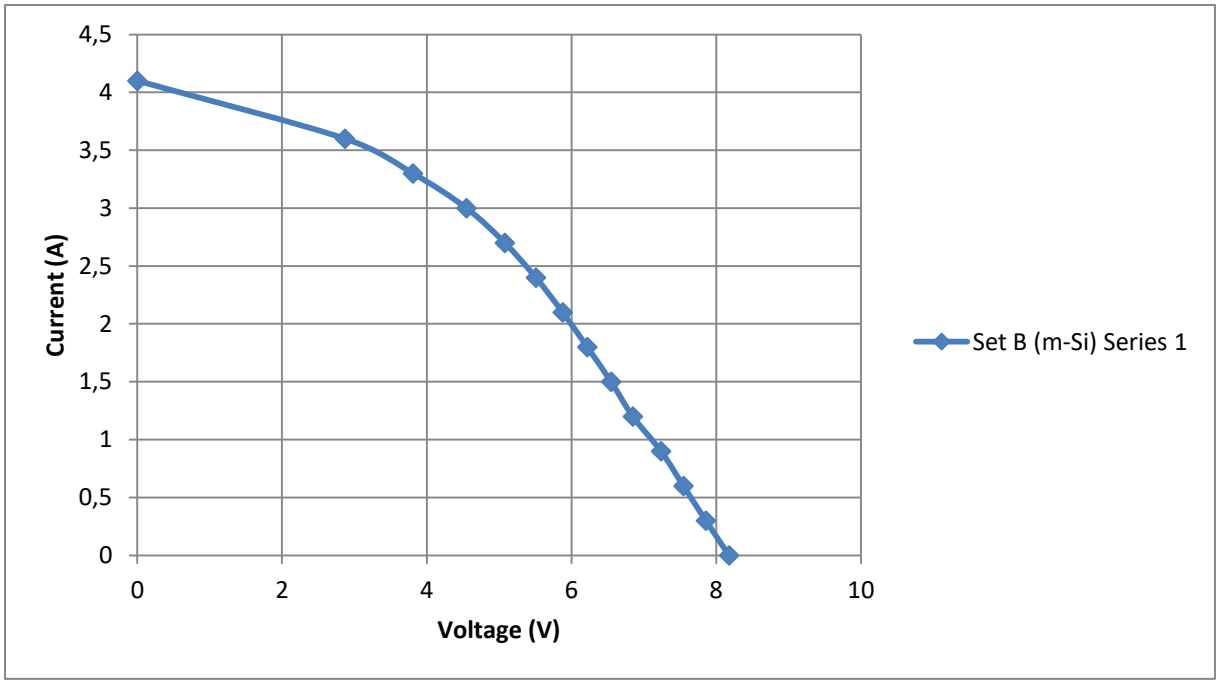

Figure 34. I-V curve for the Set B (m-si) under concentrated irradiance

The short circuit current is 4,1± 0,01 A and the open circuit is equal to 8,18± 0,01 V.

Figure 35 shows the data points and the power curve for Set B (m-si) under concentrated irradiance:

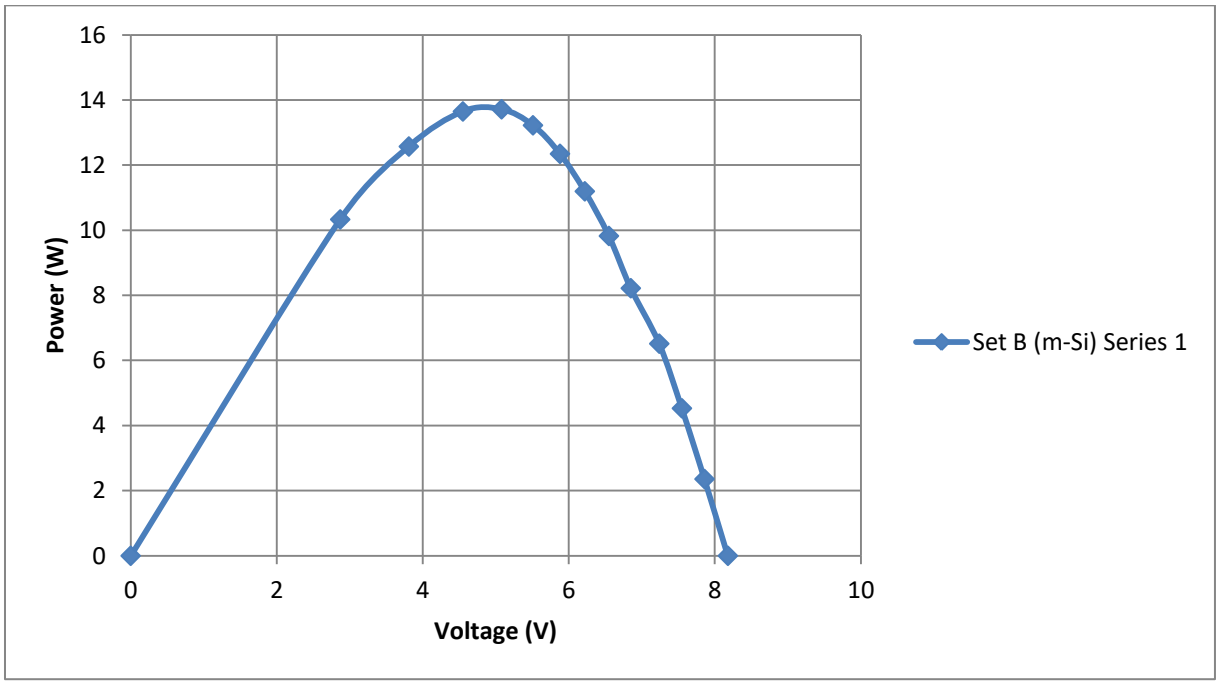

Figure 35. Power curve for Set B (m-si) under concentrated irradiance

The maximum power generated by these cells is equal to 13,72± 0,01 W.

The maximum electrical efficiency for both a-Si and m-Si cells under concentrated irradiance can also be calculated using Equation 2. The dimensions of the cells remain the same. The maximum power generated by the a-Si and m-Si cells are 5,98± 0,01 W and 13,72± 0,01 W respectively.

In order to obtain a value of concentrated irradiance, one can use Equation 6 for concentration ratio. The average value of concentration calculated based on previous results from all series is equal to 2,2. As the 1 sun irradiance was equal to 850±25 W/m^2, The concentrated irradiance is thus equal to 1870±55W/m^2.

As mentioned previously, geometrical concentration calculated using Equation 7 is equal to 4. Thus, there is a significant difference between the values obtained using Equation 6 and Equation 7. This difference may be due to the fact, that there are numerous optical errors on the surface of the mirror. Because of these errors, not all light is not directed into a focus. Furthermore, the reflexivity of the mirror may also be a factor contributing to a lower value of concentration present in the system.

The efficiency values for Set A (a-Si) and Set B (m-Si) under concentrated irradiance were calculated using Equation 2 and are equal to 6,77 ± 0,11% and 11,76 ± 0,2% respectively.

The efficiency values of Set A (a-Si) and Set B (m-Si) cells under both concentrated and non-concentrated irradiance have been gathered in Table 1:

Table 1. Maximum electrical efficiency values under concentrated and non-concentrated irradiance

	non-concentrated irradiance		concentrated irradiance	
	Set A (a-Si)	Set B (m-Si)	Set A (a-Si)	Set B (m-Si)
Maximum electrical efficiency [-]	6,90±0,12%	14,91±0,25%	6,77±0,11%	11,76±0,2%

As one can notice, the efficiency of amorphous silicon cells stayed almost identical even when the irradiance increased. However in the case of monocrystalline silicon cells a significant drop in electrical efficiency was observed. The efficiency of monocrystalline silicon cells is much more dependent on temperature than amorphous silicon. Monocrystalline silicon cells should thus not be used in CPVT systems with a high concentration ratio if a cooling system is absent. Due to increased temperature, their efficiency can drop greatly and even permanent cell damage may occur [11].

4.3 System's thermal parameters analysis

Thermal parameters are as important as electrical parameters in case of CPVT systems. Three key parameters were measured: mass flow rate, cells' temperature and water temperature.

The difference in temperature of the solar cells with and without cooling could potentially give indication of how much thermal energy was absorbed by the cells. More importantly however, cells' temperature is a key factor influencing the electrical efficiency of the cells.

Water inlet and outlet temperatures can be used to directly calculate the amount of useful heat generated by the system. These values can later be used to estimate a thermal efficiency of the CPVT collector.

First, key thermal parameters were measured under 1-sun irradiance. All measurements were performed under a clear sky with an irradiance of around 850W/m^2.

The temperature of the cells was measured using two different devices. A laser pyrometer was used to measure the temperature of distinct points on the solar cells' surface. Three points on each cell were investigated – in the middle of the cell, on the cell's side and on the cell's edge. In Figure 36 are shown the locations of these points for both monocrystalline silicon and amorphous silicon cells.

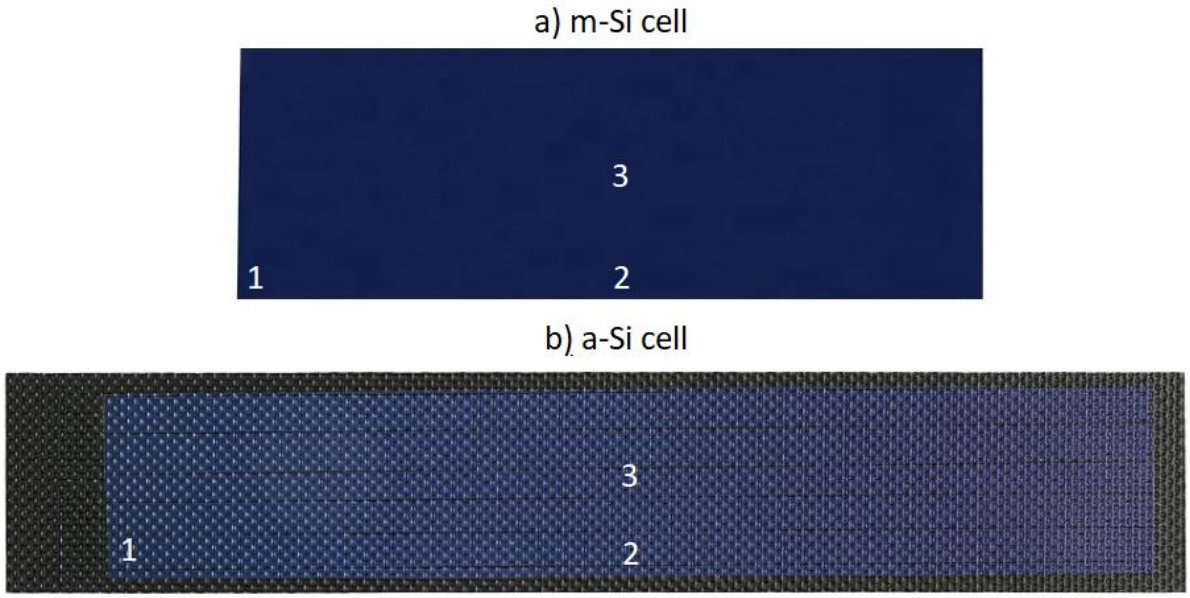

Figure 36. Measurement points locations

The measurements using the pyrometer were performed for both concentrated (with and without cooling) and non-concentrated (with and without cooling) system. Temperature analysis for the system with cooling will be discussed in subchapter 4.4.

The results for both concentrated and non concentrated system without cooling are shown in Tables 2 and 3. The values presented in the table are average temperature values calculated based on measurements for each individual cell.

Table 2. Cells' temperature under non-concentrated irradiance without cooling

	a-Si cells	m-Si cells
Point 1 temperature [°C]	50,3±0,1	49,4±0,1
Point 2 temperature [°C]	50,2±0,1	49,7±0,1
Point 3 temperature [°C]	50,3±0,1	49,8±0,1

Table 3. Cells' temperature under concentrated irradiance without cooling

	a-Si cells	m-Si cells
Point 1 temperature [°C]	84,0±0,1	82,1±0,1
Point 2 temperature [°C]	83,9±0,1	82,3±0,1
Point 3 temperature [°C]	84,3±0,1	82,3±0,1

In order to obtain more detailed results, an infra-red camera was used. The images generated by the IR camera allowed to analyze every point of the cell and a get more holistic view on the systems ' elements temperature.

However due to the fact that an IR camera is very sensitive to concentrated beams and a high concentration of reflected rays could damage the device, it was only used in the measurements of the non concentrated system for caution.

Below are shown IR camera images, thermograms and thermal analysis charts created in the Radiometric software. The emissivity of the camera was set to 0.95, ,to ensure that the most credible solar cells' temperature values will be obtained.

An exemplary thermogram showing the receiver with the a-Si cells facing sun is shown in Figure 37.

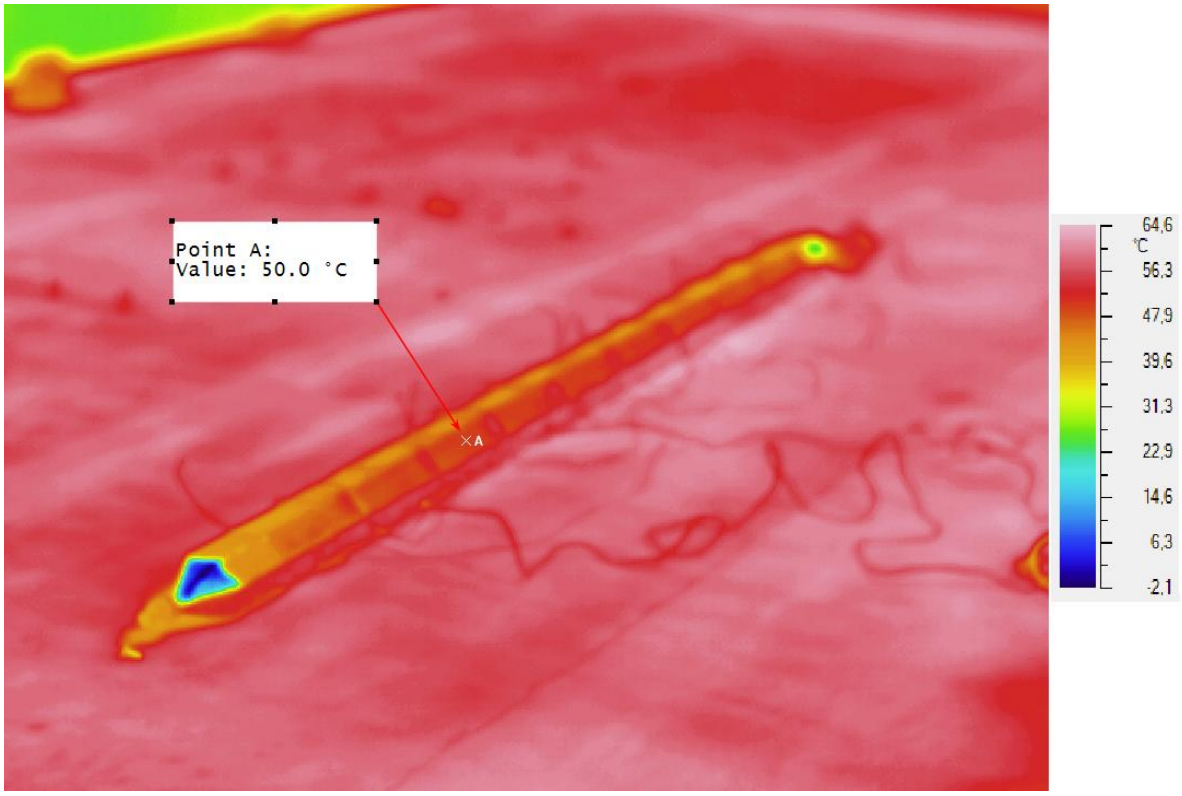

Figure 37. IR camera image – amorphous cells under 1 sun irradiance

As shown in the Figure 37, the temperature of an amorphous silicon cell in its centre is equal to 50,0°C under 1-sun irradiance. From the image and the scale, one can see that the cell's temperature is around 50°C.

One can easily notice an abnormality in the bottom left corner of the image – according to the scale, an element of the system has a temperature of around -2.0°C. This element is the part of the aluminum duct. Since the irradiance at the time of the measurement was around 850W/m^2 and the ambient temperature was well above 25°C – this element could not have had such a low temperature. There is a possible explanation for this abnormality.

The IR camera measures the heat emitted by an object or an element and converts it into an electronic signal – which allows for a calculation of a temperature. Sometimes the structure of the material can lead to an abnormal detection of the heat emitted – thus the thermogram generated can show inappropriate values of temperature. It seems to be the case here – another small abnormality can be seen in the top right corner, where the end of the duct is made of the same material and has

the same shape. Furthermore, the emissivity set to 0.95 could lead to erroneous temperature results for materials other than solar cells, since they may have different emissivity. Luckily, this part of the installation is of no concern in the thesis, thus the abnormality does not influence the results.

Basing on multiple such images, temperature distributions for a-Si and m-Si cells were determined. Even though the temperature scale in Figure 37 ranges from -2,1°C(due to the abnormality) to 64,6°C – the main concern is only the temperature of solar cells. With RADIOMETRIC – a software dedicated to performing the analyses of thermograms the areas of solar cells were isolated and temperature distributions on their surfaces were generated. The temperature distributions have been shown in Figures 38 and 39:

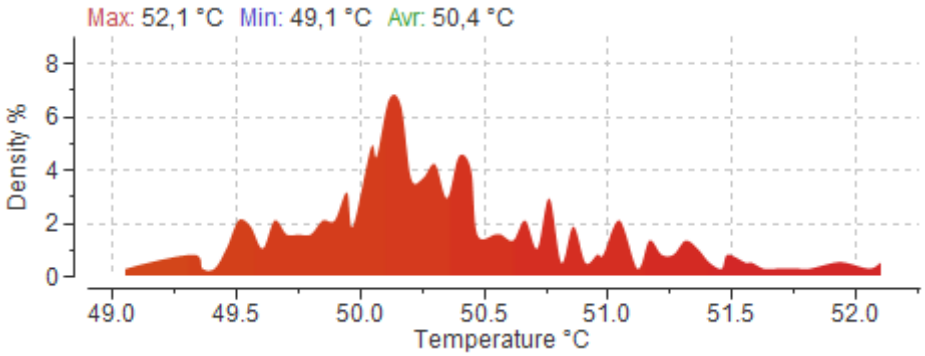

Figure 38. Temperature distribution for a-Si cells

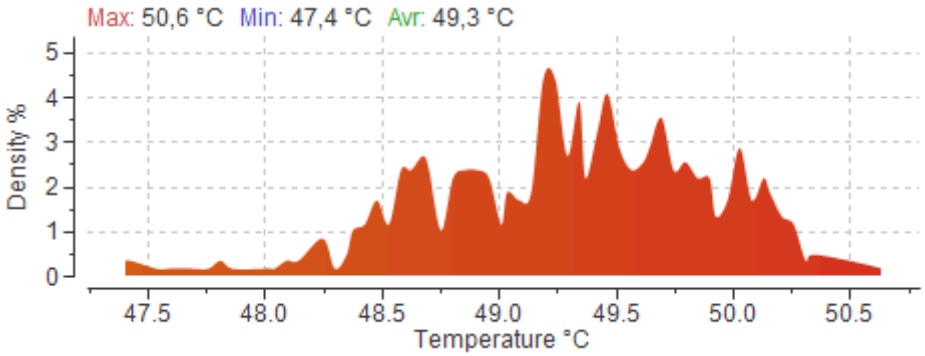

Figure 39. Temperature distribution for m-Si cells

Both amorphous silicon and monocrystalline silicon cells achieved a temperature of around 50°C under 1-sun irradiance. Overall, a-Si cells' temperature was slightly higher than a-Si cells' with the average of 50,4°C to 49,3°C respectively. The highest percentage of the a-Si cells area achieved between 50,0°C and 50,5°C, while in the case of m-Si cells it was mostly between 49,0°C and 50,0°C.

These values can be compared with calculations allowing to estimate a temperature of solar cells under given conditions. In order to calculate the temperature of the cell, Equation 3 was applied.

The NOCT for monocrytalline silicon and amorphous silicon cells can be assumed to be equal to 45°C and 47°C respectively according to the literature [17]. The ambient temperature during the measurements was equal to 27°C. Air temperature was measured using an ambient air thermometer, which was located in a close vicinity to the CPVT collector. The temperature values were taken down every 20 minutes, on average it was 27°C with only 1-2°C deviation.

Using the Equation 3, the m-si cell temperature should be equal to 54°C under 1-sun irradiance, and 85°C under concentrated irradiance. In the case of a-si cells, these temperatures should be equal to 56°C and 90°C respectively.

This simplified model only gives approximate temperature values and does not represent the reality accurately. Nevertheless, the values obtained using Equation 3 are quite accurate when compared to direct measurements with a pyrometer or an IR camera.

There are a number of factors that lead to the differences between the values obtained using these methods. Even though wind speed was small most of the time, even small disturbances in the wind speed could potentially influence the temperature of the cells. The temperature of the roof was much higher than the ambient temperature, and since the cells were located near the roof for some time, it could also influence the cells' temperature. Finally, even though the measurements were performed in a short period of time to keep ambient conditions constant, it was impossible to ensure that no fluctuations appear – and any changes in irradiance and ambient temperature had a direct effect on the cells' temperature.

Then, inlet and outlet water temperatures were measured for a non-concentrated system. Two values of water flow were investigated – 2 l/min and 4 l/min.

Total amount of thermal power generated could be calculated using Equation 4. All data and results for both m-Si and a-Si cells under non-concentrated irradiance can be found in Table 4. Inlet and outlet temperature values in the table were averaged based on 3 measurements.

Table 4. Water temperature and heat generated by the system under non-concentrated irradiance

	a-Si cells		m-Si cells	
	flow [2l/min]	flow 4[l/min]	flow [2l/min]	flow 4[l/min]
inlet temperature [°C]	29,8±0,1	27,2±0,1	29,6±0,1	28,2±0,1
outlet temperature [°C]	31,6±0,1	28,5±0,1	31,5±0,1	29,3±0,1
temperature difference [°C]	1,8±0,1	1,3±0,1	1,9±0,1	1,1±0,1
Thermal power generated [W]	252±14	364±28	266±14	308±28

Given the results, it was determined that a high flow of 4 l/min lead to the generation of more heat than the flow of 2 l/min. Because of that, for the analysis of the concentrated system, only the flow of 4 l/min was investigated and analyzed.

The temperature values as well as amount of heat generated in the case where the irradiance was being concentrated can be found in Table 5.

Table 5. Water temperature and heat generated by the system under concentrated irradiance

	a-Si cells	m-Si cells
	flow 4[l/min]	flow 4[l/min]
inlet temperature [°C]	27,5±0,1	27,6±0,1
outlet temperature [°C]	29±0,1	29,1±0,1
temperature difference [°C]	1,5±0,1	1,5±0,1
Thermal power generated [W]	420±28	420±28

Concentrated irradiance increased the temperature difference when compared to the non-concentrated system results. Since the temperature difference is a key element in calculating the heat generated by the system, using a concentrating mirror increased the useful heat obtained by the installation.

The solar to thermal efficiency can be calculated using Formula 5, as well as the data and results obtained in this section. For the calculations it was assumed that the non-concentrated beam is perpendicular to the top wall of the receiver and the concentrated beam is perpendicular to the bottom wall of the receiver. With this assumption, for 4 remaining walls the effective area which receives the irradiance needs to be multiplied by the cosine of 60˚. Given that, total solar power received by the receiver can be calculated as follows:

$$P_{solar} = 1 \cdot 2\text{m} \cdot 0.05\text{m} \cdot 850 \pm 25\frac{\text{W}}{\text{m}^2} + 2 \cdot 2\text{m} \cdot 0.05\text{m} \cdot \cos 60° \cdot 850 \pm 25\frac{\text{W}}{\text{m}^2} +$$

$$1 \cdot 2\text{m} \cdot 0.05\text{m} \cdot 2.2 \cdot 850 \pm 25\frac{\text{W}}{\text{m}^2} + 2 \cdot 2\text{m} \cdot 0.05\text{m} \cdot \cos 60 \bullet \cdot 2.2 \cdot 850 \pm 25\frac{\text{W}}{\text{m}^2} = 544 \pm 16\text{W}$$

Solar to heat efficiency under concentrated irradiance was calculated with Equation 5 and is equal to 77,20±6,09%.

4.4 Combined operation of electricity and heat generating components

In case of CPVT systems it is paramount to understand how electricity and heat generating components operate simultaneously. Increased irradiance due to the presence of a concentrator leads to a greater electrical energy output, however because of higher cells' temperature, electrical efficiency decreases. Furthermore, depending on a number of factors, such as the materials out of which solar cells are made, as well as thermal conductivity of the receiver's wall – thermal efficiency of the CPVT collector can vary.

In this part of the analysis, both electrical and thermal parameters were measured and these results were compared to previous values obtained in subchapters 4.2 and 4.3. Having collected all necessary data, one can calculate the overall efficiency of the system and understand how heat and electricity generating components cooperate.

First, I-V and power curves of the cells under 1-sun with cooling for both Set A (a-si) and Set B (m-si) were plotted. Set A (a-si) curves can be found in Figures 40 and 41:

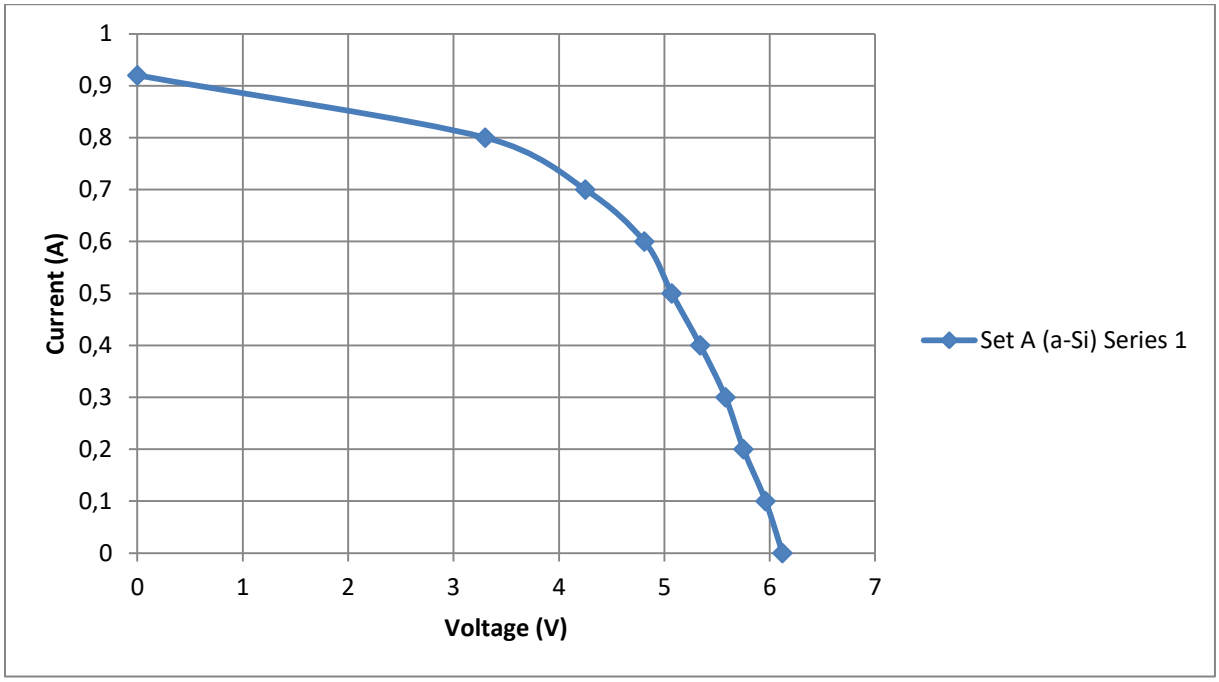

Figure 40. I-V curve for Set A (a-si) under non-concentrated irradiance with cooling

The short circuit current is equal to around 0,91± 0,01 A, while the open circuit voltage to around 6,1± 0,01 V.

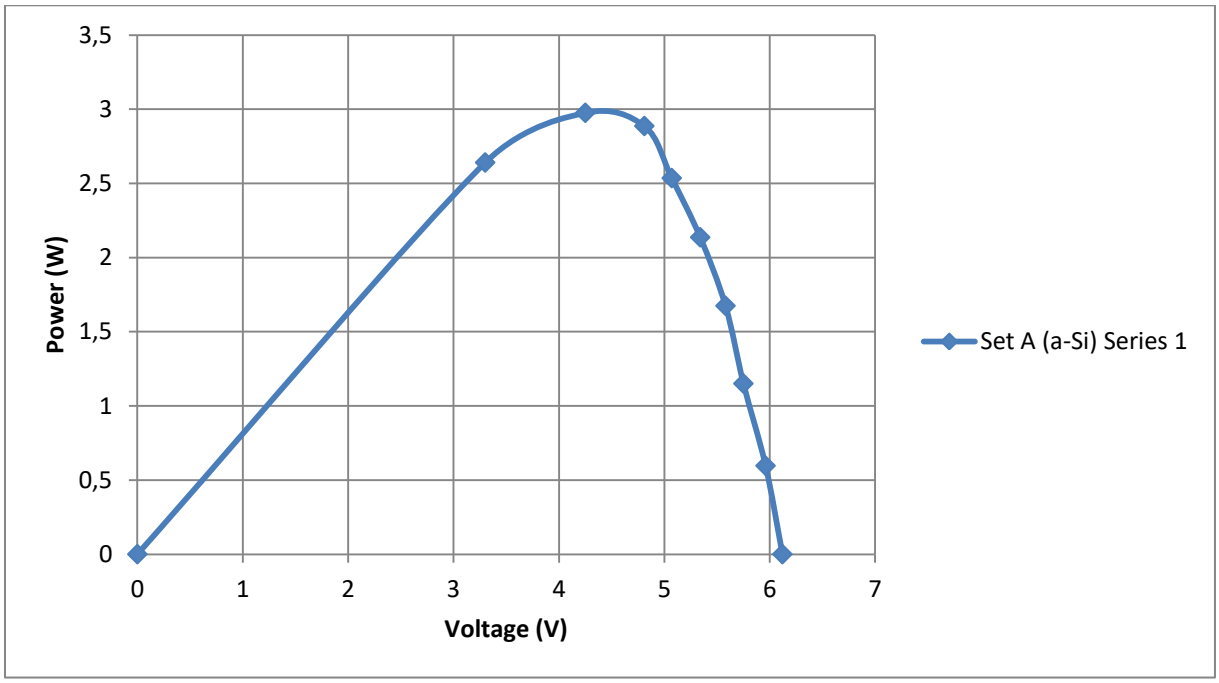

Figure 41. Power curve for Set A (a-si) under non-concentrated irradiance with cooling

The highest maximum power was equal to 2,99± 0,01 W. The maximum power is thus slightly larger than in the case where no cooling was used.

Analogical curves were plotted for Set B (m-si) and are shown in Figures 42 and 43.

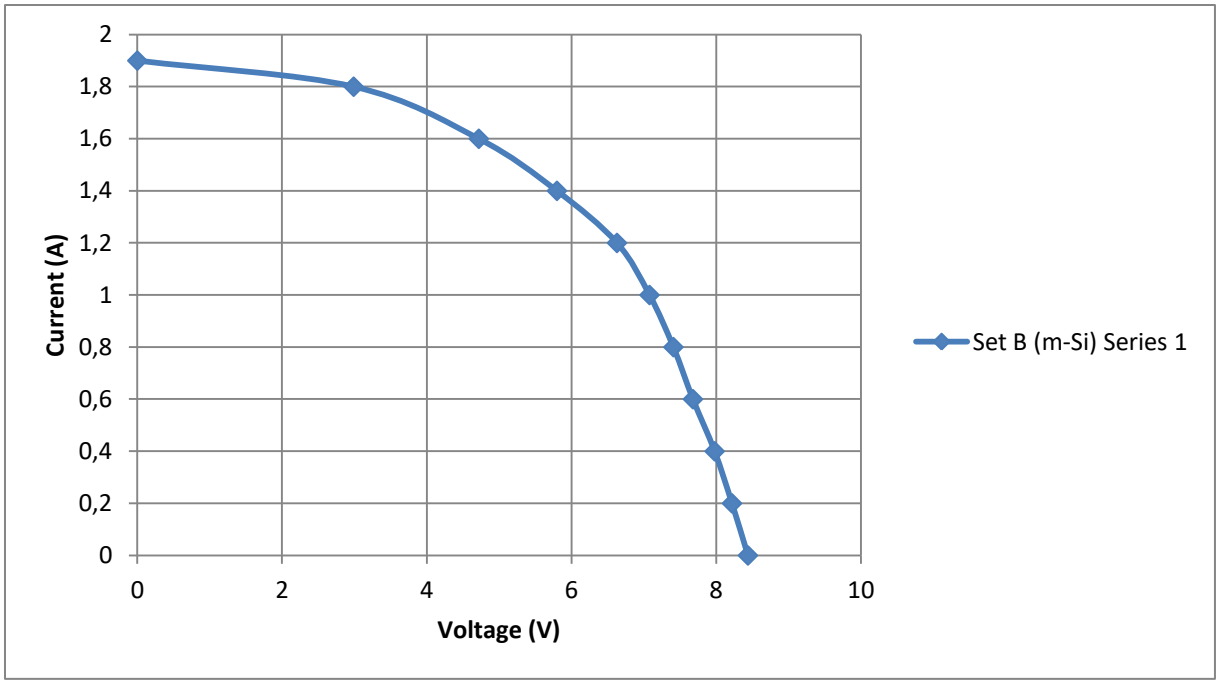

Figure 42. I-V curve for Set B (m-si) under non-concentrated irradiance with cooling

The short circuit current is equal to 1,9± 0,01 A, while the open circuit voltage to 8,4± 0,01 V.

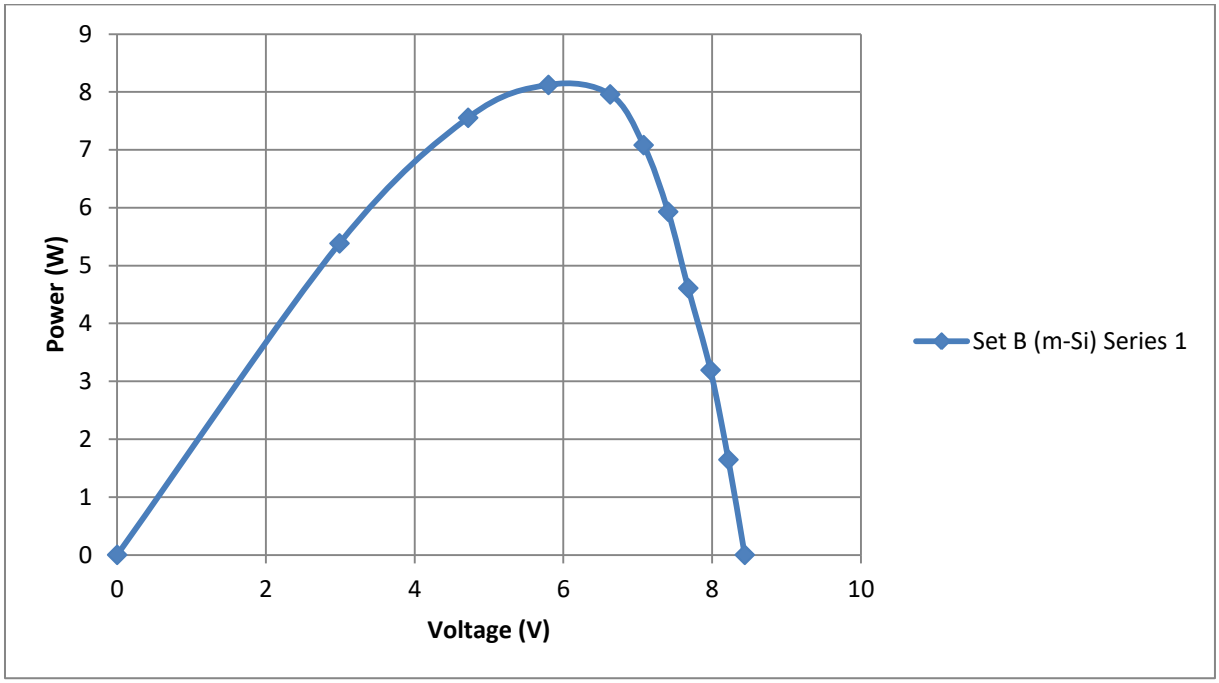

Figure 43. Power curve for Set B (m-si) under non-concentrated irradiance with cooling

The highest maximum power was equal to 8,08± 0,01 W. The maximum power is thus slightly larger than in the case where no cooling was.

As one can see, when compared to a scenario where the cells were not cooled, maximum power is larger. The short circuit current remains almost the same, while the open circuit voltage increases slightly. It has to do with the water cooling the cells down which leads to the increase of the electrical parameters.

Then, the measurements were performed when the sunlight was being concentrated onto the receiver. The electrical parameters – the I-V and power curves - obtained under concentrated light with cooling for Set A (a-si) and Set B (m-si) are shown in Figures 44 and 45:

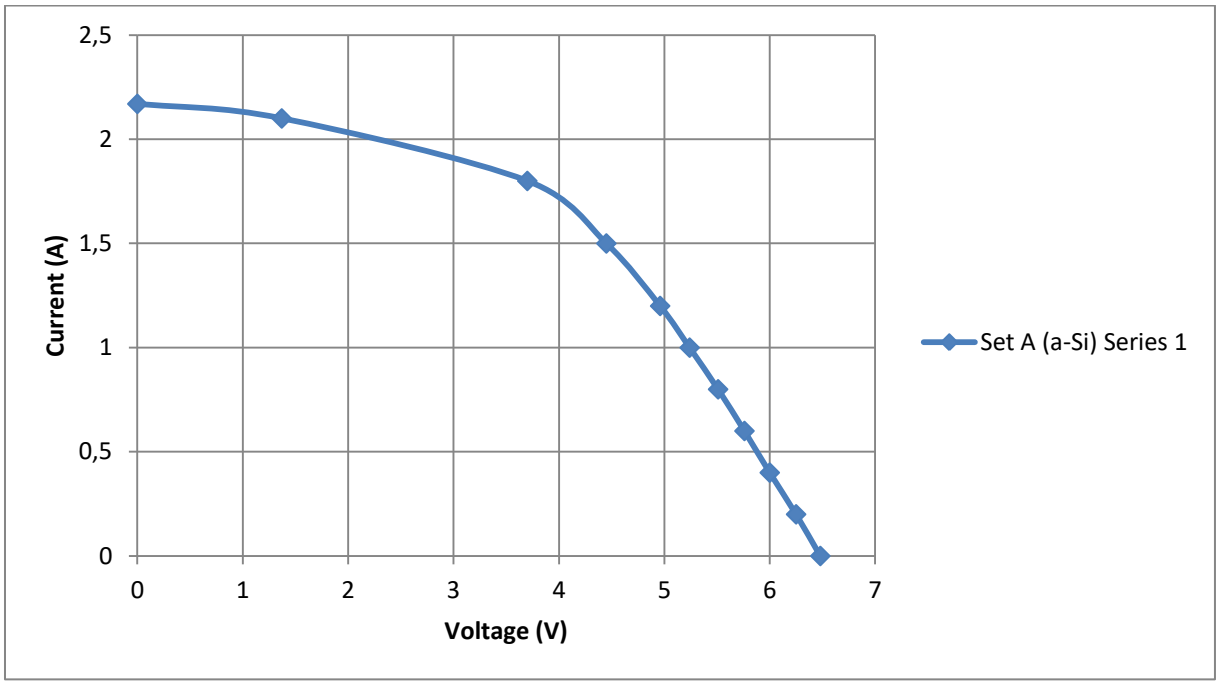

Figure 44. I-V curve for Set A (a-si) under concentrated irradiance with cooling

The short circuit current is equal to 2,15± 0,01 A, while the open circuit voltage to around 6,5± 0,01 V.

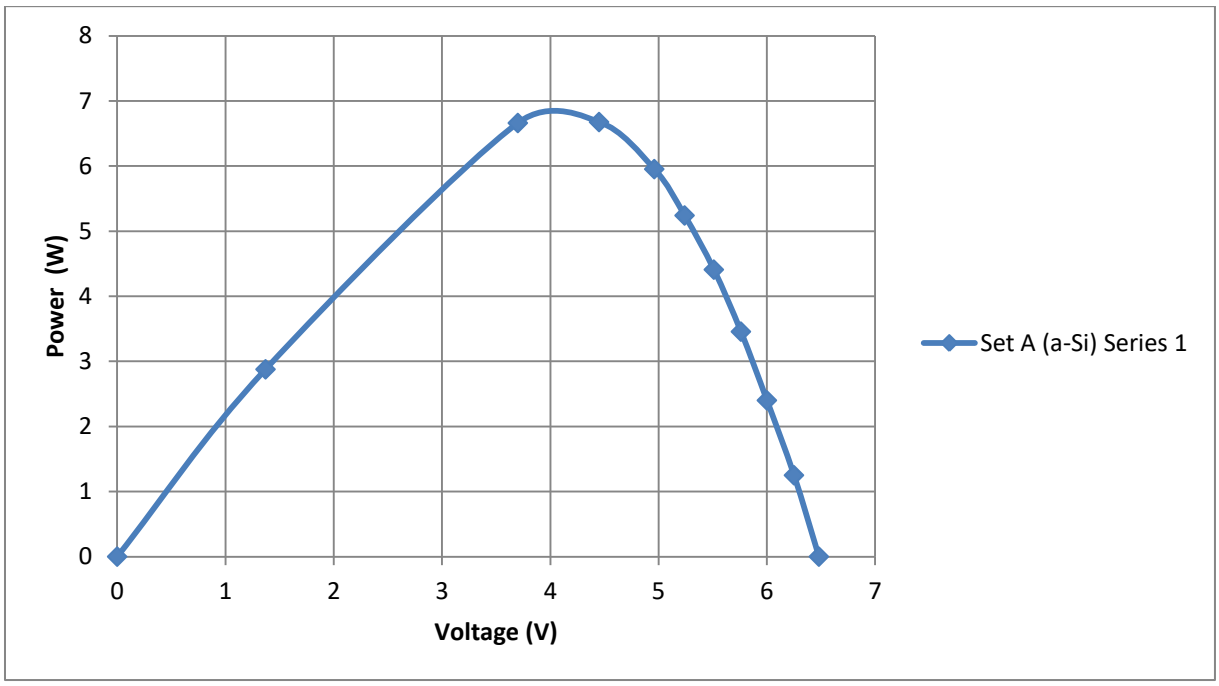

Figure 45. Power curve for Set A (a-si) under concentrated irradiance with cooling

The maximum power was equal around to 6,8± 0,01 W.

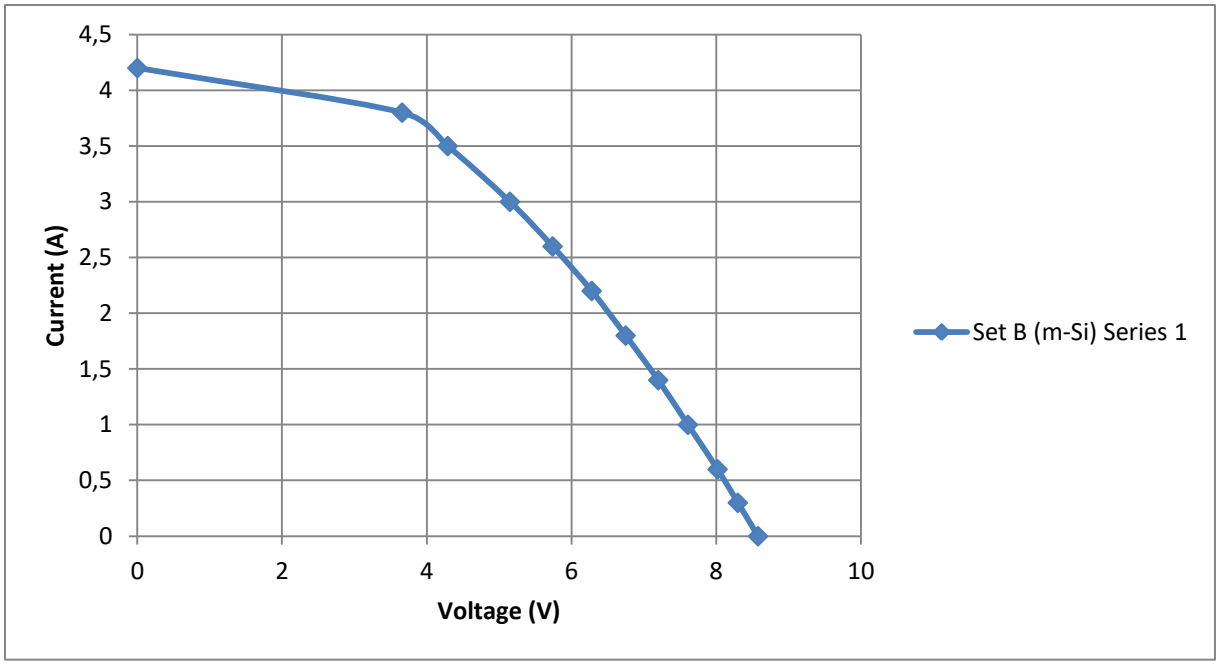

Figure 46. I-V curve for Set B (m-si) under concentrated irradiance with cooling

The short circuit current is equal to 4,2± 0,01 A, while the open circuit voltage to 8,4± 0,01 V.

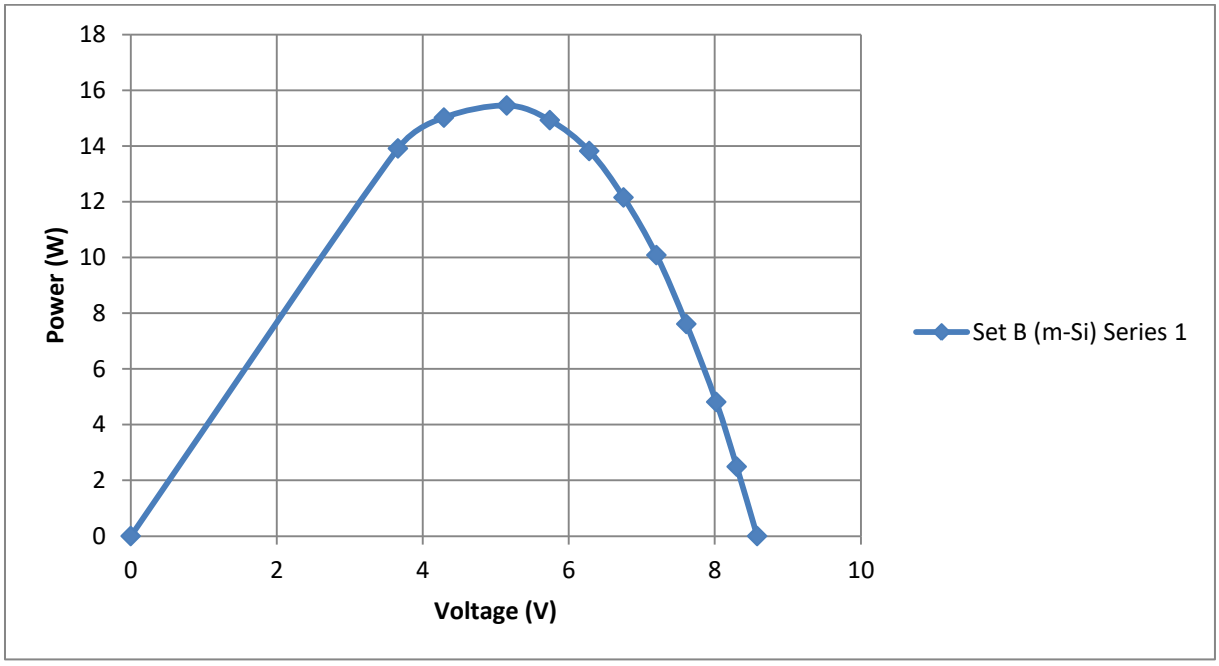

Figure 47. Power curve for Set B (m-si) under concentrated irradiance with cooling

The maximum power was equal to 15,8± 0,01 W.

In order to have a full picture of all measurements performed the thesis, I-V and power curves for four scenarios were plotted on individual charts. The relationship between different conditions and the results is thus clearly visible.

The best results for the following four scenarios were compared between one another:

S1: Without concentration, without cooling

S2: With Concentration, without cooling

S3: With concentration, with cooling

S4: Without concentration, with cooling

Figures 48 and 49 show the I-V and power curves for all scenarios above.

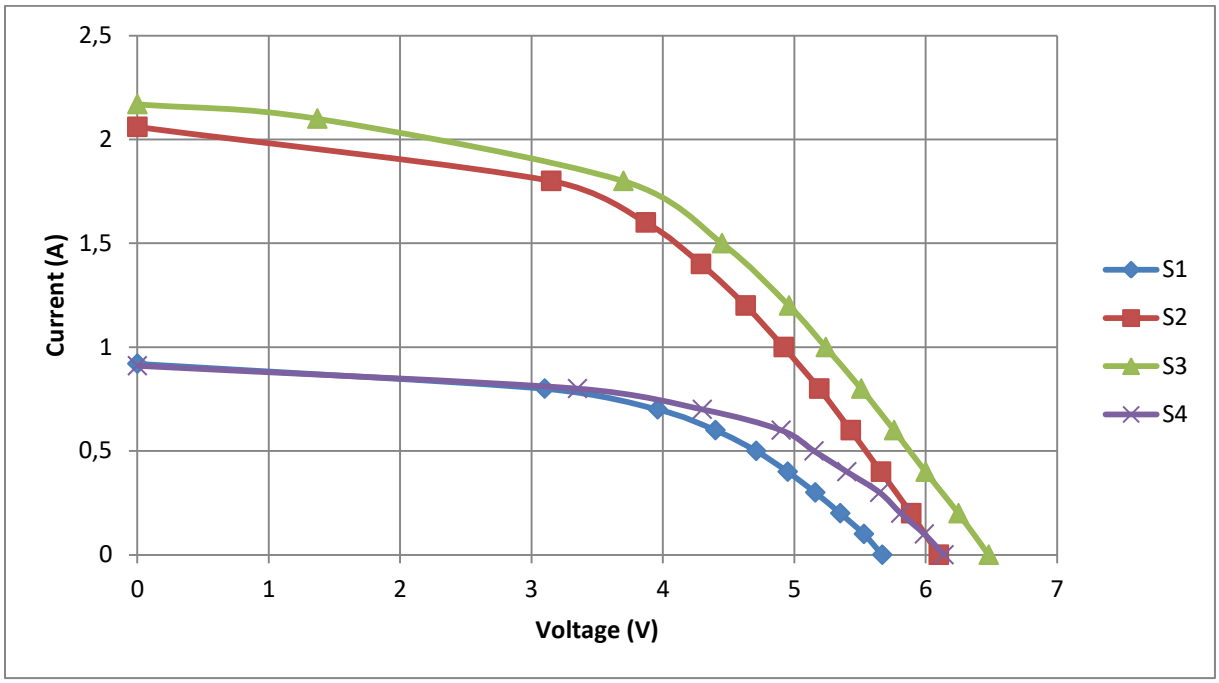

Figure 48. I-V curve for chosen scenarios for Set A (a-si)

Under 1-sun irradiance short circuit current remains nearly identical. It has to do with the fact, that the irradiance was almost identical, thus no major changes in the I_{sc} were noticed. The open circuit voltage however is noticeably higher in the case where cooling was used.

In the case of concentrated irradiance, a slight difference in I_{sc} between a cooled and not cooled system can be seen. It might have to do with the fact, that the cells' temperature decreased in S3. There is around 2˚C difference between the temperature of cells in each case.

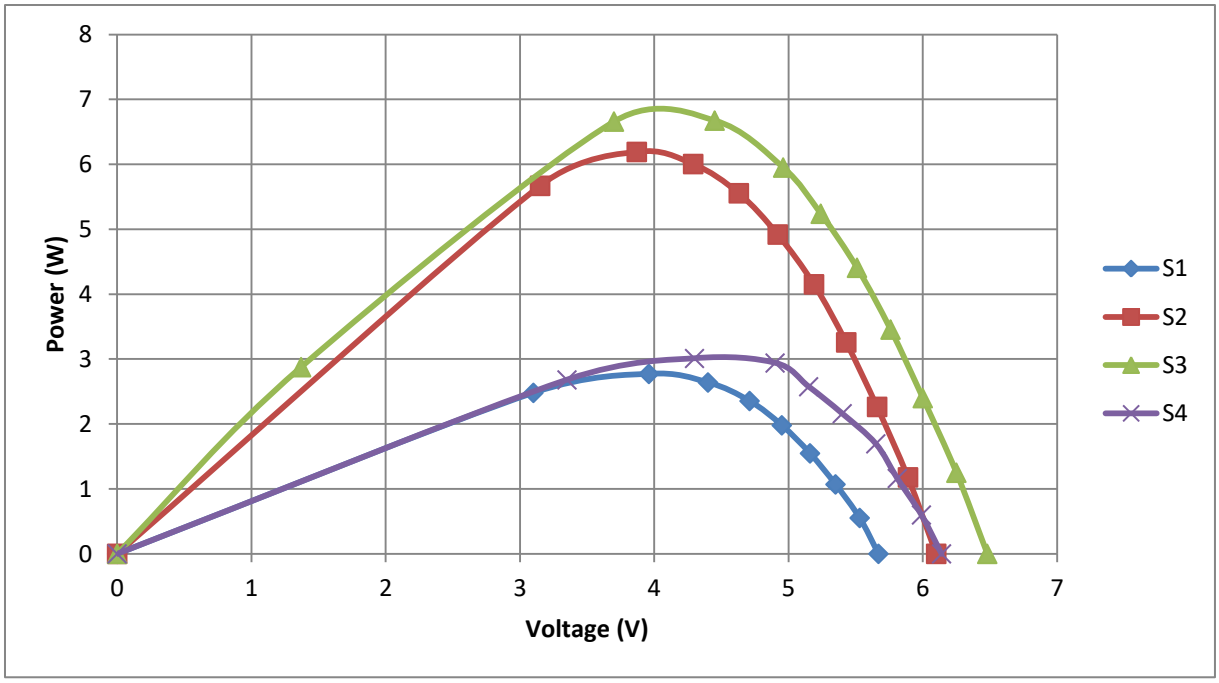

Figure 49. Power curve for chosen scenarios for Set A (a-si)

One can easily notice that the highest maximum power is generated when the sunlight is concentrated and cooling is used. The lowest energy output is obtained with 1-sun irradiance by the system without cooling. When these two scenarios are compared, it turns out that in the first case, over twice as much energy can be obtained.

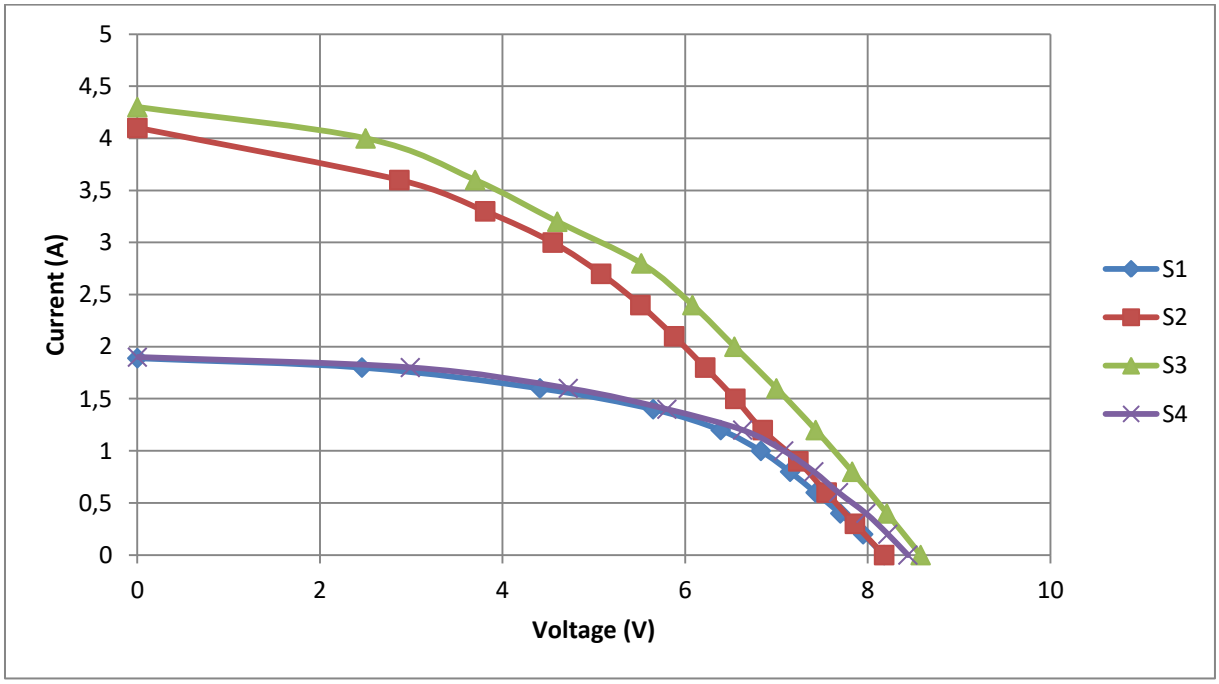

Figure 50. I-V curve for chosen scenarios for Set B (m-si)

Similar relationships to the ones for a-Si cells are present in the case of m-Si cells as well and are shown in Figures 50 and 51.

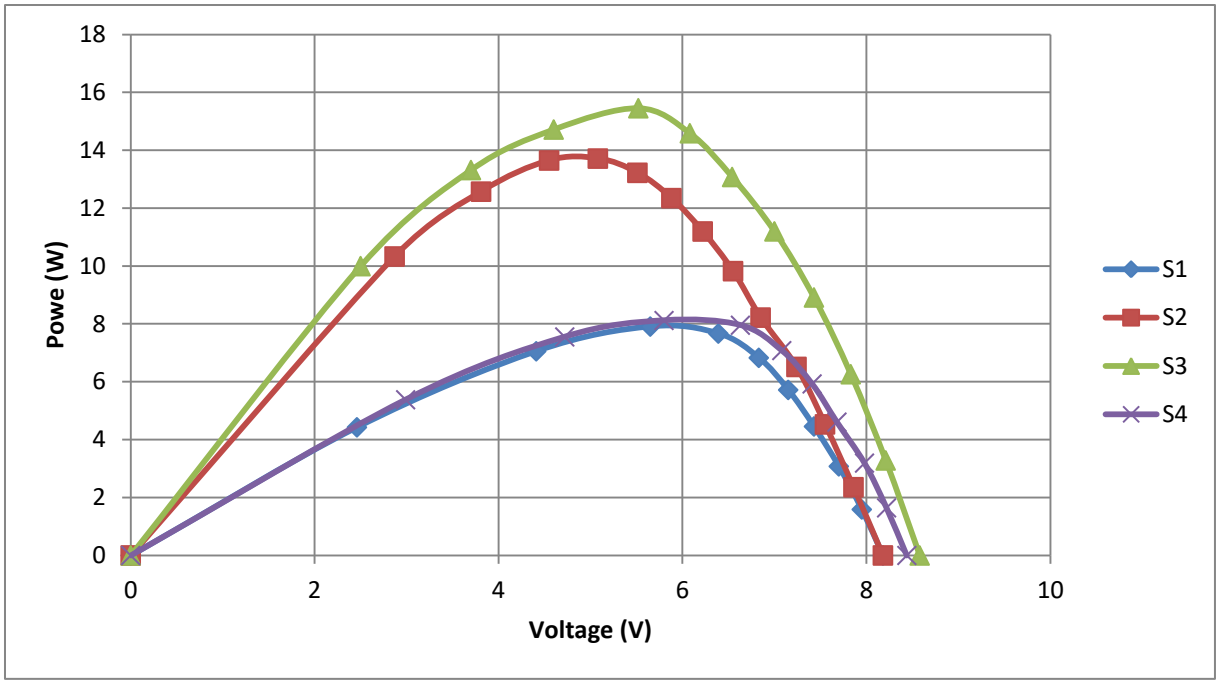

Figure 51. Power curve for chosen scenarios for Set B (m-si)

Similarly to the a-Si cells, the highest energy is generated under concentrated irradiance with cooling, while the lowest energy – under 1-sun irradiance without cooling. When comparing these two scenarios, around twice as much energy can be generated when both cooling and a concentrator are used.

The temperature values of the distinct points of the cells measured with the pyrometer are shown in Table 6:

Table 6. Cells' temperature under concentrated irradiance with cooling

	a-Si cells	m-Si cells
Point 1 temperature [°C]	82,0±0,1	80,1±0,1
Point 2 temperature [°C]	81,9±0,1	80,3±0,1
Point 3 temperature [°C]	82,1±0,1	80,2±0,1

When compared to the cells temperature values without cooling, a noticeable decrease can be noticed. The decrease of the cells temperature leads to the increase of an open circuit voltage, as shown in figures 48 and 50.

Inlet and outlet temperature as well as heat generated by the system under concentrated irradiance with cooling can be found in Table 7:

Table 7. Water temperature and heat generated by the system under concentrated irradiance

	a-Si cells	m-Si cells
	flow 4[l/min]	flow 4[l/min]
inlet temperature [°C]	27,5±0,1	27,6±0,1
outlet temperature [°C]	29±0,1	29,1±0,1
temperature difference [°C]	1,5±0,1	1,5±0,1
Thermal power generated [W]	420±28	420±28

In order to maximize the energy output of the installation, all 6 walls of the receiver should be equipped with solar cells. With the results obtained in previous sections, total energy output and system efficiency when solar cells are attached to all walls of the receiver can be calculated.

Two cases will be investigated: (1) equipping the receiver fully with a-Si cells and (2) equipping the receiver fully with m-Si. All calculations are performed based on the equations mentioned in previous parts of the thesis. Table 8 contains information regarding the efficiency and the amount of power generated in both cases.

Table 8. Systems efficiency and energy output values

	amorphous silicon cells	monocrystalline silicon cells
Electrical power generated [W]	19.58±0,01	47,6±0,01
Thermal power generated [W]	420±28	420±28
Electrical efficiency [-]	7,69±0,14%	13,54±0,24%
Thermal efficiency [-]	77,20±6,09%	77,20±6,09%

There is a great difference between the amount of electrical power generated between a-Si and m-Si cells. Monocrystalline silicon cells have a much greater efficiency than amorphous silicon cells, hence when the output energy and electrical efficiency is of paramount importance – m-Si cells are preferred. Both heat generated and thermal efficiency are equal regardless of the technology of cells used. Thermal efficiency values exceed the results found in literature, however it has to do with the fact, that thermal losses are very low due to a low temperature increase. Electrical efficiency values are decent and comparable to other similar prototype installations found in the literature.

For instance, a low concentration CPVT system with Fresnel lenses built by Kong et al. achieved electrical and thermal efficiencies of 10% and 56% respectively [46]. Thermal and electrical efficiencies of a CPVT system manufactured by Bernardo et al. were measured to be equal to 45% and 6.4% [47]. Brogren et al. developed a CPVT installation with parabolic concentrators with a total efficiency of 71% [47].

5. Conclusions and future work

In the scope of the thesis a prototype CPVT collector was constructed and analyzed. As the result of the analysis it was possible to determine the power generated and efficiency achieved by the system. It was determined that if all walls of the receiver were equipped with solar cells, a satisfactory efficiency can be achieved. Thermal efficiency of around 77%, is higher than most systems described in literature. Electrical efficiencies of around 7,7% and 13,54% (depending on which solar cells were used) is comparable with similar prototype devices described in literature [46][47][48].

Some prototype CPVT collectors with monocrystalline solar cells were reported to achieve thermal efficiency as high as 58% [31]. Other systems, using GaAs cells reached thermal efficiencies of 35-42% [31]. When it comes to electrical efficiency, a water-cooled CPVT system using monocrystalline silicon cells described in literature achieved electrical efficiency of 11% [31].

However, the amount of useful heat and electricity generated is too low for a system of this size to compete with conventional solar panels and solar collectors. It will thus most likely not find any commercial uses, but can certainly be a valuable experimental installation for research.

The experimental results show that the higher the irradiance, the higher the electrical power generated by the CPVT collector. Concentrating irradiance leads to the increase of a short circuit current, but keeps the open circuit voltage on almost the same level. However, the higher the irradiance, the higher the cells temperature – and it leads to the decrease of the cells' efficiency. The results showed, that monocrystalline silicon cells' efficiency is much more sensitive to sunlight than amorphous silicon cells' efficiency.

It was determined that the heat is efficiently recovered by the cooling fluid, with thermal efficiency exceeding 70%. The use of the cooling fluid also leads to a noticeable decrease of the solar cells' temperature thus improving the electrical efficiency of the cells. The reason the thermal efficiency of the CPVT collector investigated in this thesis is so high, is that working fluid temperatures are low, which significantly decreases thermal losses in the system.

A number of improvements can be applied in order to increase the system's output power and efficiency. By equipping every wall of the receiver one maximizes energy output that can be obtained – and this way was investigated in the thesis. It is also possible to investigate the use of other solar cells, such as modern, highly-efficient thin-film cells.

Thermal efficiency could be further increased by choosing receiver materials with higher thermal conductivity. More research might be needed to investigate the fluid flow and find an optimal flow that leads to maximum thermal efficiency under given conditions. All of these ideas can be implemented in future work with the installation.

Since solar energy is becoming more popular all over the world and new solar technologies are being developed, there is an enormous potential for the future work.

References

[1] Bauers A., Menrad K. (2019). Standing up for the Paris Agreement: Do global climate targets influence individuals' greenhouse gas emissions? Environmental Science and Policy, 99(2019), 72-79.

[2] Manabe S. (2019). Role of greenhouse gas in climate change. Dynamic Meteorology and Oceanography, 71(1), 1-13.

[3] www.epa.gov – access 20.04.2022.

[4] www.irena.org – access 20.04.2022.

[5] Murphy C., Gardoni P., McKim R. (2018). Climate Change and Its Impacts - Risks and Inequalities. Cham: Springer Nature.

[6] Krost C. et al. (2021). Levelized Cost of Electricity - Renewable Energy Technologies. Fraunhofer Institute for Solar Energy Systems ISE.

[7] Chaanaoui M., Vaudreuil S., Bounahmidi T. (2016). Benchmark of Concentrating Solar Power Plants: Historical, Current and Future Technical and Economic Development. Procedia Computer Science, 83(2016), 782-789.

[8] www.ec.europa.eu – access 24.04.2022.

[9] Vissarionov V. et al. (2008). Solnechnaya Energetika, Moscow: Izdatel'sky Dom MEI.

[10] Lewandowski W. (2006). Proekologiczne odnawialne źródła energii. Warsaw: Wydawnictwo Naukowo-Techniczne.

[11] Foster R., Ghassemi M., Cota A. (2010). Solar Energy: Renewable Energy and the Environment. Boca Raton: Taylor and Francis Group LLC.

[12] Klugmann-Radziemska E. (2010): Fotowoltaika w teorii i praktyce. Legionowo: Wydawnictwo BTC.

[13] Chen C. J. (2011). Physics of Solar Energy, Hoboken: John Wiley & Sons INC.

[14] Callister W. D., Rethwisch D. G. (2010) Materials Science and Engineering – an Introduction, Hoboken: John Wiley & Sons INC.

[15] Patel M. R., (1999). Wind and Solar Power Systems. Boca Raton: CRC Press LLC.

[16] Szymański B. (2014). Instalacje fotowoltaiczne. Cracow: Geosystem Burek Kotyza S.C.

[17] Sun V. et al. (2021). Evaluation of nominal operating cell temperature (NOCT) of glazed photovoltaic thermal module. Case Studies in Thermal Engineering, 28(2021), 1-15.

[18] Jastrzębska G. (2014). Ogniwa słoneczne – Budowa, technologie i zastosowanie. Warsaw: Wydawnictwo Komunikacji i Łączności.

[19] Letcher T. M. (2014). Future Energy: Improved, Sustainable and Clean Options for our Planet. London: Elsevier Ltd.

[20] Lovegrove K. (2021). Concentrating Solar Power Technology: Principles, Developments and Applications. London: Elsevier Ltd.

[21] Smets A. et al. (2016). Solar Energy – the physics and engineering of photovoltaic conversion technologies and systems. Cambridge: UIT Cambridge Ltd.

[22] Himer S. E. et al. (2020): Photovoltaic Concentration: Research and Development, Energies 13(2020), 1-41.

[23] Garrido S. G. et al. (2012). Guía técnica de la energía Solar Termoeléctrica. Madrid: Fundación de la Energía de la Comunidad de Madrid.

[24] International Energy Agency. (2010). Technology Roadmap - Concentrating Solar Power. Paris: IEA.

[25] Heller P. (2017). The Performance of Concentrated Solar Power (CSP) Systems – Analysis, Measurement and Assessment. London: Elsevier.

[26] Chandra L. (2018). Concentrated Solar Thermal Energy Technologies - Recent Trends and Applications. Singapore: Springer Nature.

[27] Mokhtar M. et al. (2015). Direct Steam Generation for Process Heat using Fresnel Collectors. The International Journal of Thermal & Environmental Engineering, 10(1), 3-9.

[28] Zondag H. A. (2008). Flat-plate PV-Thermal collectors and systems - a review. Renewable and Sustainable Energy Reviews, 12(4), 893-959.

[29] Daneshazarian R. (2018). Concentrating photovoltaic thermal (CPVT) collectors and systems: Theory, performance assessment and applications. Renewable and Sustainable Energy Reviews, 81(2018), 473–492.

[30] Fırat C. (2021). Electrical and Thermal Performance Analysis of a Linear Fresnel Reflector Photovoltaic/Thermal System. Academic Platform Journal of Engineering and Science, 9(2), 264-273.

[31] Karathanassis, I.K. et al. (2017). Design and experimental evaluation of a parabolic-trough concentrating photovoltaic/thermal (CPVT) system with high-efficiency cooling. Renewable Energy, 101(C), 467-483.

[32] Kibria M. T. et al. (2015). A Review: Comparative studies on different generation solar cells technology, Proceedings of 5th International Conference on Environmental Aspects of Bangladesh.

[33] Daneshazarian R. (2017). An Overview of Concentrating Photovoltaic Thermal (CPVT) Collectors. Energy Research Journal, 8(1), 11-21.

[34] https://www.nrel.gov/ - Access: 06.01.2022

[35] Kraynov A. (2016). Osnovy Teploperedachi - Teploperedacha Cherez Sloy Veshchestva. Tomsk: Izdatel'stvo "STT".

[36] Chow T.T. (2010) A review on photovoltaic/thermal hybrid solar technology. Applied Energy, 87(2), 365-379.

[37] Sharaf O. Z., Orhan M. F. (2015). Concentrated photovoltaic thermal (CPVT) solar collector systems: Part II – Implemented systems, performance assessment, and future directions, Renewable and Sustainable Energy Reviews, 50(2015), 1566-1633.

[38] www5.biall.com.pl - Access: 27.10.2021

[39] www.fluke.com - Access: 22.04.2022

[40] www.test-therm.pl/ - Access: 22.04.2022

[41] – www.archiwumalle.pl - Access: 27.10.2021

[42] www.sterlingsensors.co.uk- Access: 22.04.2022

[43] www.benning.de - Access: 22.04.2022

[44] www.flowquip.co.uk - Access: 22.04.2022

[45] www.codesys.com - Access: 22.04.2022

[46] Kong C., Xu Z., Yao Q. (2013). Outdoor performance of a low-concentrated photovoltaic-thermal hybrid system with crystalline silicon solar cells, Applied Energy, 112(2013), 618-625.

[47] Bernardo L. R. et al. (2011). Performance evaluation of low concentrating photovoltaic/thermal systems: a case study from Sweden, Solar Energy, 85(2011), 1499-1510.

[48] Brogren M., Nostell P., Karlsson B. (2000). Optical efficiency of a PV thermal hybrid CPC module for high latitudes, Solar Energy, 69(2000), 173-185.